FOURIER TRANSFORM ION CYCLOTRON RESONANCE MASS SPECTROMETRY: A PRIMER

Alan G. Marshall,*† Christopher L. Hendrickson, and George S. Jackson†

Center for Interdisciplinary Magnetic Resonance, National High Magnetic Field Laboratory, Florida State University, 1800 East Paul Dirac Dr., Tallahassee, FL 32310

Received 7 January 1998; revised 4 May 1998; accepted 6 May 1998

Mass Spectrometry Reviews, **1998,** *17*, 1–35

CCC 0277-7037/98/010001-35

This review offers an introduction to the principles and generic applications of FT-ICR mass spectrometry, directed to readers with no prior experience with the technique. We are able to explain the fundamental FT-ICR phenomena from a simplified theoretical treatment of ion behavior in idealized magnetic and electric fields. The effects of trapping voltage, trap size and shape, and other nonidealities are manifested mainly as perturbations that preserve the idealized ion behavior modified by appropriate numerical correction factors. Topics include: effect of ion mass, charge, magnetic field, and trapping voltage on ion cyclotron frequency; excitation and detection of ICR signals; mass calibration; mass resolving power and mass accuracy; upper mass limit(s); dynamic range; detection limit, strategies for mass and energy selection for MS^n; ion axialization, cooling, and remeasurement; and means for guiding externally formed ions into the ion trap. The relation of FT-ICR MS to other types of Fourier transform spectroscopy and to the Paul (quadrupole) ion trap is described. The article concludes with selected applications, an appendix listing accurate fundamental constants needed for ultrahigh-precision analysis, and an annotated list of selected reviews and primary source publications that describe in further detail various FT-ICR MS techniques and applications. © 1998 John Wiley & Sons, Inc., Mass Spec Rev 17, 1–35, 1998

I. INTRODUCTION

Fourier transform ion cyclotron resonance mass spectrometry (FT-ICR MS or FTMS) is widely practiced (more than 235 installations worldwide by 1998). In the 24 years since its inception (Comisarow and Marshall, 1974; Comisarow and Marshall, 1974), FT-ICR MS has been the sole or principal subject of three books, four journal special issues, and more than 60 review articles (see Appendix A). However, the various prior descriptions and reviews are distributed among dozens of primary publications with different formalism and notation, and those articles are directed mainly at FT-ICR MS practitioners. Here, we present an introduction to the principles and generic applications of FT-ICR MS, at the minimum depth needed to explain the concepts, directed to those without prior experience in the field.

Fortunately for beginners, it turns out that many fundamental aspects of FT-ICR can be understood from very simple idealized models. First, ion cyclotron frequency, radius, velocity, and energy as a function of ion mass, ion charge, and magnetic field strength follow directly from the motion of an ion in a spatially uniform static magnetic field. Second, ion cyclotron motion may be rendered spatially coherent (and thus observable) by the application of a spatially uniform rf electric field (excitation) at the same frequency as (i.e., ''resonant'' with) the ion cyclotron frequency. The ICR (time-domain) signal results from induction (detection) of an oscillating ''image'' charge on two conductive infinitely extended opposed parallel electrodes. A frequency-domain spectrum (convertible to a mass-domain spectrum) is obtained by Fourier transformation of the digitized time-domain ICR signal. Third, confinement of ions by the application of a three-dimensional axial quadrupolar d.c. electric field shifts the ion cyclotron frequency, whereas excitation and detection remain essentially linear (i.e., doubling the excitation amplitude doubles the detected ICR signal) but with a reduced proportionality constant. A simple mass calibration rule follows from this treatment. Thus, FT-ICR MS may be performed in essentially the same way in ion traps of widely different shape (e.g., cubic, cylindrical). Fourth, collisions broaden the ICR signal in a simple way, and actually make it possible to cool and compress an ion packet for improved detection (and even multiple remeasurement). Fifth, although FT-ICR MS has been coupled to virtually every type of ion source, most ion sources work best (or at least most conveniently) outside the magnet. Thus, several methods have been developed to guide externally generated ions into an ion trap inside a high-field magnet. Finally, the above features may be combined in various experimental ''event sequences'' (much like pulse sequences in FT-NMR spectroscopy) to perform tandem-in-time mass spectrometry (MS/MS, or MS^n).

II. ION CYCLOTRON MOTION: ION CYCLOTRON ORBITAL FREQUENCY, RADIUS, VELOCITY, AND ENERGY

An ion moving in the presence of a spatially uniform magnetic field, $\boldsymbol{B} = -B_0\mathbf{k}$ (i.e., the z-axis is defined as the direction opposite to B) is subject to a force given (in S.I. units) by Eq. (1),

$$\text{Force} = \text{mass} \cdot \text{acceleration} = m\frac{d\boldsymbol{v}}{dt} = q\boldsymbol{v} \times \boldsymbol{B} \qquad (1)$$

in which m, q, and $\boldsymbol{v}$ are ionic mass, charge, and velocity,

* Correspondence to: Professor Alan G. Marshall, Director, Ion Cyclotron Resonance Program, National High Magnetic Field Laboratory, Florida State University, 1800 East Paul Dirac Drive, Tallahassee, FL 32310.
† Department of Chemistry, Florida State University, Tallahassee, FL.
Contract grant sponsors: NSF, N.I.H., NSF National High Field FT-ICR Mass Spectrometry Facility, Florida State University, National High Magnetic Field Laboratory.
Contract grant nos.: CHE-93-22824, GM-31683, CHE-94-130081

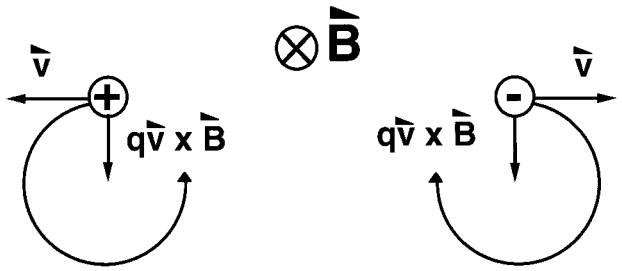

FIGURE 1. Ion cyclotron motion. The path of an ion moving in the plane of the paper is bent into a circle (see text) by the inward-directed Lorentz magnetic force produced by a magnetic field directed perpendicular to the plane of the paper. Note that positive and negative ions orbit in opposite senses. Reproduced with permission from (Marshall and Grosshans, 1991).

and the vector cross product term means that the direction of the magnetic component of the Lorentz force is perpendicular to the plane determined by $\boldsymbol{v}$ and $\boldsymbol{B}$. If the ion maintains constant speed (i.e., no collisions), then the magnetic field bends the ion path into a circle of radius, r (see Fig. 1).

Let $v_{xy} = \sqrt{v_x^2 + v_y^2}$ denote the ion velocity in the xy plane (i.e., the plane perpendicular to **B**). Because angular acceleration, $|dv/dt| = v_{xy}^2/r$, Eq. (1) becomes

$$\frac{mv_{xy}^2}{r} = qv_{xy}B_0. \tag{2}$$

But angular velocity, ω (in rad/s), about the z-axis is defined by

$$\omega = \frac{v_{xy}}{r} \tag{3}$$

so that Eq. (2) becomes

$$m\omega^2 r = qB_0\omega r,$$

or simply

$$\omega_c = \frac{qB_0}{m} \quad \text{(S.I. units)} \tag{4a}$$

$$\boxed{\nu_c = \frac{\omega_c}{2\pi} = \frac{1.535611 \times 10^7 B_0}{m/z}}$$

$$\left(\begin{array}{c}\nu_c \text{ in Hz; } B_0 \text{ in tesla; } m \text{ in u;}\\ z \text{ in multiples of elementary charge}\end{array}\right). \tag{4b}$$

Equation (4) is the celebrated ''cyclotron'' equation, in which the ''unperturbed'' ion cyclotron frequency is denoted as ω_c. A remarkable feature of Eq. (4) is that all ions of a given mass-to-charge ratio, m/q, have the same ICR frequency, *independent of their velocity*. This property makes ICR especially useful for mass spectrometry, because translational energy ''focusing'' is not essential for the precise determination of m/q.

Several useful conclusions follow directly from Eq. (4). First, at a representative static magnetic field value of 7.0 tesla (at which the corresponding proton NMR Larmor frequency would be 300 MHz), ICR frequencies for ions formed from typical molecules range from a few kHz to a few MHz (see Fig. 2)—a very convenient range for commercially available electronics.

Rearrangement of Eq. 2 yields the *ion cyclotron orbital radius*,

$$r = \frac{mv_{xy}}{qB_0} \quad \text{(S.I. units)} \tag{5a}$$

$$\boxed{r = \frac{1.036427 \times 10^{-8}\,(\text{m/z})\, v_{xy}}{B_0}}$$

$$\left(\begin{array}{c}r \text{ in m; } v_{xy} \text{ in m/s; } B_0 \text{ in tesla; } m \text{ in u;}\\ z \text{ in multiples of elementary charge}\end{array}\right). \tag{5b}$$

of an ion of velocity, v_{xy}. For example, the average x–y translational energy of an ion in equilibrium with its surroundings at temperature, T (in K), is given by

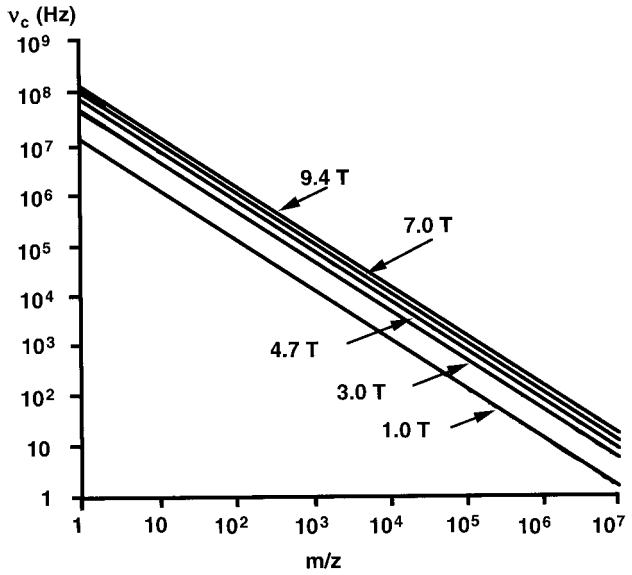

FIGURE 2. ICR orbital frequency, $\nu_c = \omega_c/2\pi$, in Hz, as a function of ionic mass-to-charge ratio, m/z, in Daltons per multiple (z) of the elementary electron charge, at each of five magnetic field strengths: 1.0, 3.0, 4.7, 7.0, and 9.4 tesla. Note that ICR frequencies for ions in the usual ''chemical'' mass-to-charge ratio range ($\sim 15 \leq m/z \leq 10{,}000$) typically lie between a few kHz and a few MHz.

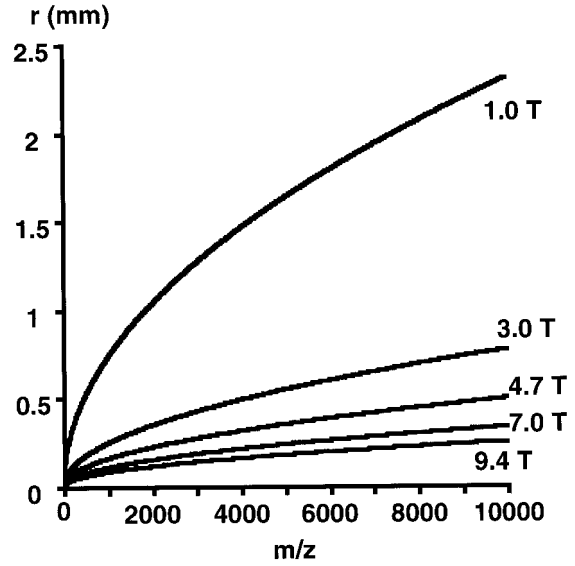

FIGURE 3. ICR orbital radius, r [Eq. (7)], vs. ionic mass-to-charge ratio, m/z (in u per multiple of elementary electronic charge) at each of five representative magnetic field strengths: 1.0, 3.0, 4.7, 7.0, and 9.4 tesla at 298 K. Note that even relatively heavy ions are confined to conveniently small-radius orbits by such magnetic fields.

$$\frac{m\langle v_{xy}^2\rangle}{2} \approx kT \tag{6}$$

in which k is the Boltzmann constant. Solving Eq. (6) for v_{xy}, and substituting back into Eq. (5), we obtain

$$r = \frac{1}{qB_0}\sqrt{2\,mkT} \quad \text{(S.I. units)} \tag{7a}$$

$$\boxed{r = \frac{1.336510 \times 10^{-6}}{zB_0}\sqrt{mT}}$$

$$\left(\begin{array}{c} r \text{ in m; } B_0 \text{ in tesla; } m \text{ in u; } T \text{ in K;} \\ z \text{ in multiples of elementary charge} \end{array}\right). \tag{7b}$$

The reader can quickly confirm that at room temperature, a singly charged ion of m = 100 u in a magnetic field of 3 tesla (i.e., 30,000 Gauss) has an ICR orbital radius of ~0.08 mm. At room temperature, a singly charged ion of mass, 10,000 u, has an ICR orbital radius of only ~0.8 mm, whereas a singly charged ion of 50,000 u has an ICR orbital radius of 1 cm. Thus, ions of thermal energy formed from all but the largest molecules are confined by the magnetic field to conveniently small orbital radii for ICR excitation and detection (see Fig. 3).

Conversely, we can compute the *velocity* and *translational energy* of an ion excited (by as yet unspecified means) to a larger-than-thermal orbital radius. From Eq. (5),

$$v_{xy} = \frac{qB_0r}{m} \quad \text{(S.I. units)} \tag{8a}$$

$$v_{xy} = \frac{9.64853 \times 10^7 B_0 r}{(m/z)}$$

$$\left(\begin{array}{c} v_{xy} \text{ in m/s; } r \text{ in m; } B_0 \text{ in tesla; } m \text{ in u;} \\ z \text{ in multiples of elementary charge} \end{array}\right). \tag{8b}$$

From Eq. (8), a singly charged ion of 100 u mass excited to an ICR orbital radius of 1 cm in a magnetic field of 3 tesla has a translational velocity, v_{xy} = 2.97 $\times 10^4$ m/s, that corresponds to a translational energy,

$$\text{Kinetic energy} = \frac{mv_{xy}^2}{2} = \frac{q^2B_0^2r^2}{2m} \quad \text{(S.I. units)} \tag{9a}$$

$$\boxed{\text{K.E.} = \frac{4.824265 \times 10^7 z^2 B_0^2 r^2}{m}}$$

$$\left(\begin{array}{c} \text{energy in eV; } r \text{ in m; } B_0 \text{ in tesla; } m \text{ in u;} \\ z \text{ in multiples of elementary charge} \end{array}\right). \tag{9b}$$

of 434 eV. Thus, ions can be ''heated'' to high translational energy even in a relatively small container, and induced to break into smaller fragments by collision with neutral gas molecules (see below). The dependence of ion kinetic energy on ICR orbital radius and magnetic field strength is shown in Fig. 4.

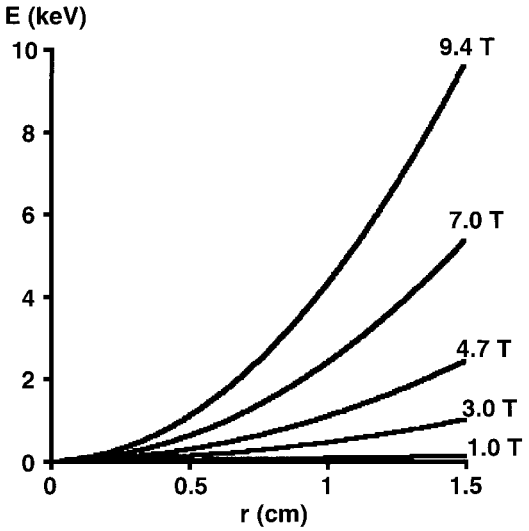

FIGURE 4. Ion translational (kinetic) energy [Eq. (9)] as a function of ICR orbital radius, at each of five common magnetic field strengths: 1.0, 3.0, 4.7, 7.0, and 9.4 tesla, for an ion of m/z = 100. Note that ions may be accelerated to relatively high energy (≥1 keV, as in collision-induced dissociation experiments) while still confined to relatively small (~1 cm) orbital radii (compare to previous figure).

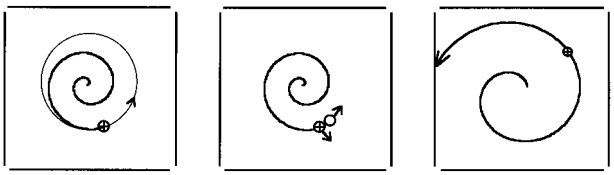

FIGURE 5. Uses for ion cyclotron excitation. Left: Acceleration of ions to form a spatially coherent packet at detectable orbital radius. Middle: Increase in ion kinetic energy to above the threshold for collision-activated dissociation or reaction. Right: Ejection of ions of a given mass-to-charge ratio.

Finally, it is instructive to note that the excited ion of 100 u of the preceding paragraph travels a distance of ~30 kilometers during a 1-s observation period! That's basically why ICR offers potentially much higher mass resolution than even a several-meter-long magnetic-sector ''beam'' instrument.

III. EXCITATION AND DETECTION OF AN ICR SIGNAL

A. Azimuthal Dipolar Single-Frequency Excitation

Ion cyclotron motion is not by itself useful. Virtually all applications are, therefore, based on *excitation* produced by applying a spatially uniform electric field oscillating (or rotating) at or near the cyclotron frequency of ions of a particular *m*/*z* value. Excitation is used in three ways in FT-ICR MS (see Fig. 5): (a) to accelerate ions coherently to a larger (and thus detectable) orbital radius; (b) to increase ion kinetic energy above the threshold for ion dissociation and/or ion–molecule reaction; and (c) to accelerate ions to a cyclotron radius larger than the radius of the ion trap (see below), so that ions are removed (''ejected'') from the instrument.

Next let us apply an azimuthal (i.e., in a plane perpendicular to **B**) spatially uniform electric field, $\boldsymbol{E}(t)$, oscillating sinusoidally with time along the +/−*y*-direction.

$$\boldsymbol{E}(t) = E_0 \cos\, \omega_c t\mathbf{j} \tag{10}$$

in which **i** and **j** denote unit vectors along the *x*- and *y*-axes. For now, we shall suppose that E_0 is generated by applying $+V_0$ and $-V_0$ volts to two opposed infinitely extended parallel conductive flat plates separated by *d* meters, so that

$$E_0 = \frac{2V_0}{d} = \frac{V_{p\text{-}p}}{d} \tag{11}$$

in which $V_{p\text{-}p}$ is the peak-to-peak voltage difference between the two plates (see Fig. 6).

This linearly polarized electric field may be analyzed into two counter-rotating components, $\boldsymbol{E}_L(t)$ and $\boldsymbol{E}_R(t)$,

$$\boldsymbol{E}(t) = \boldsymbol{E}_L(t) + \boldsymbol{E}_R(t) \tag{11a}$$

in which

$$\boldsymbol{E}_R(t) = \frac{E_0}{2} \cos\, \omega t\mathbf{j} + \frac{E_0}{2} \sin\, \omega t\mathbf{i}, \tag{11b}$$

$$\boldsymbol{E}_L(t) = \frac{E_0}{2} \cos\, \omega t\mathbf{j} - \frac{E_0}{2} \sin\, \omega t\mathbf{i}. \tag{11c}$$

The radiofrequency electric field component, $\boldsymbol{E}_R(t)$, rotating in the same sense (namely, counterclockwise in the *xy*-plane) and at the same frequency (i.e., ''in resonance with'') the ion of interest pushes that ion continuously forward in its orbit, as shown in the left-hand diagram of Fig. 7. The electric field component, $\boldsymbol{E}_L(t)$, rotating in the opposite sense as the ion, is off-resonance by 2ω and has virtually no significant net effect after several cycles of the excitation frequency.

An ion absorbs power, $A(t)$, according to the dot product

$$A(t) = \text{Force} \cdot \text{velocity} = q\boldsymbol{E}(t) \cdot \boldsymbol{v}_{xy}. \tag{12}$$

For a positive (or negative) ion (initially at rest) subjected to oscillating resonant excitation [Eqs. (10), (11)] for a period, T_{excite}, it is straightforward to show from Eq. (12) that the post-excitation ion cyclotron radius, *r*, is given by

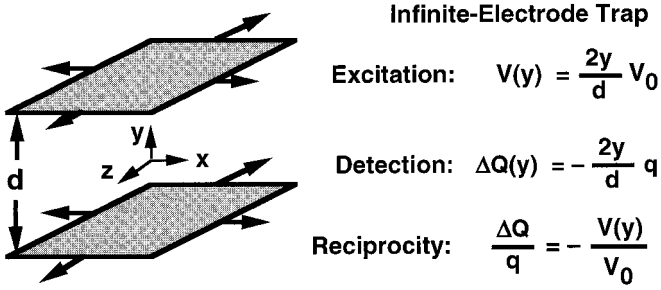

FIGURE 6. Excitation voltage difference and detection-induced charge difference in FT-ICR MS, demonstrated for two infinitely extended parallel flat electrodes located at $y = \pm d/2$ m away from the *z*-axis. If a potential $V_0 = V_{p\text{-}p}/2$ is applied to the upper electrode and $-V_0$ to the lower electrode, the potential, $V(y)$, anywhere between the electrodes is $2\ V_0 y/d$. If a point charge, *q*, is located between the same electrodes (in the absence of any applied voltage), then the difference, $\Delta Q(y)$, between the charge induced on the upper and lower electrodes is $-2\ qy/d$. It turns out that the relationship, $\Delta Q/q = -V/V_0$, is true [by the principle of ''reciprocity,'' also known as Earnshaw's theorem (Scott, 1959)] for opposed electrodes of arbitrary shape.

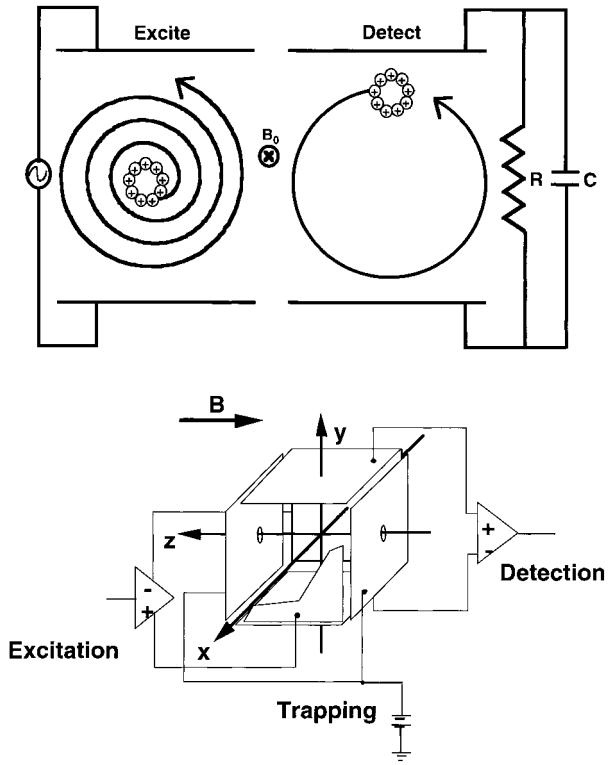

FIGURE 7. Incoherent ion cyclotron orbital motion (top left) is converted to coherent (and, therefore, detectable) motion (top right) by the application of a rotating electric field, which rotates in the same sense and at the ICR frequency of the ions of a given *m*/*z* value. The electronic circuitry is shown in the bottom diagram.

(Guan and Marshall, 1996; Schweikhard and Marshall, 1993)

$$r = \frac{E_0 T_{\text{excite}}}{2B_0} \tag{13a}$$

or

$$\boxed{r = \frac{V_{p-p} T_{\text{excite}}}{2dB_0}} \quad \text{(S.I. units).} \tag{13b}$$

A particularly delightful feature of Eq. (13) is that *post-excitation ion cyclotron orbital radius is independent of m*/z! Thus, all ions of a given *m*/*z*-range can be excited to the *same* ICR orbital radius, by application of an rf electric field whose magnitude is *constant with frequency*—i.e., no mass discrimination results from excitation, in the limit of a perfectly spatially uniform rf electric excitation field. For example, an ion of arbitrary *m*/*z* in a magnetic field of 7.0 tesla can be excited to a radius of 0.72 cm in 1.0 ms by a constant rf resonant oscillating voltage of +/−1 volt ($2V_{p\text{-}p}$) applied to infinitely extended parallel flat electrodes 2 cm apart. Thus, ions can be excited to detectably useful ICR orbital radius (i.e., to a cyclotron radius large compared to the ion initial room-temperature thermal cyclotron radius) by a relatively small rf voltage.

From Eq. (13), the ion kinetic energy immediately following azimuthal dipolar resonant excitation for a period, $T_{\text{excit'n}}$, is given by (remember that $\omega_c = qB_0/m$)

$$\text{K.E.}_{\text{post-excit'n}} = \frac{m\omega_c^2 r^2}{2} = \frac{q^2 E_0^2 (T_{\text{excite}})^2}{8m}$$

$$= \frac{q^2 V_{p\text{-}p}^2 (T_{\text{excite}})^2}{8d^2 m} \tag{14a}$$

$$\boxed{\text{K.E.}_{\text{post-excit'n}} = \frac{1.20607 \times 10^7 z^2 V_{p-p}^2 (T_{\text{excite}})^2}{d^2 m}} \tag{14b}$$

in which energy is in eV; $V_{p\text{-}p}$ is in volts; $T_{\text{excit'n}}$ is in s; *d* is in m; *m* is in u; and *z* is in multiples of elementary charge. For example, for an ion of 100 u, excited by +/−1 volt applied for 1 ms to infinitely extended parallel flat electrodes 2 cm apart, the post-excitation ion kinetic energy is 1.2 keV. Thus, it is relatively easy to generate high collision energy (see below) in an ion cyclotron. Equation (14) shows that, for a given excitation electric field amplitude and duration, *post-excitation ion kinetic energy* is *independent of magnetic field strength*, B_0. However, the post-excitation cyclotron radius [Eq. (13)] varies inversely with B_0, so that, for a given post-excitation ion cyclotron *radius*, the post-excitation ion energy increases as B_0^2 (Marshall and Guan, 1996). Post-excitation ion kinetic energy as a function of ion mass is shown in Fig. 8 for either a fixed post-excitation radius at several different magnetic field values, or a fixed excitation amplitude but several different excitation periods.

B. Azimuthal Dipolar Single-Frequency Detection

It is important to recognize that ICR orbital motion does not by itself generate an observable electrical signal (namely, a net difference between the charge induced in two opposed parallel electrodes). At its instant of formation in (or injection into) the ion trap, the *phase* of each ion's orbital motion is random—i.e., an ion may start its cyclotron motion at any point around either circle shown in Fig. 1. Thus, for an ensemble of ions, any charge induced in either of two opposed detector plates will be balanced, on the average, by an equal charge induced by an ion whose phase is 180° different (i.e., an ion located on the ''far'' side of the same orbit), so that the net difference in detected charge between the two plates is zero. Moreover, the cyclotron radius of thermal ions is too small

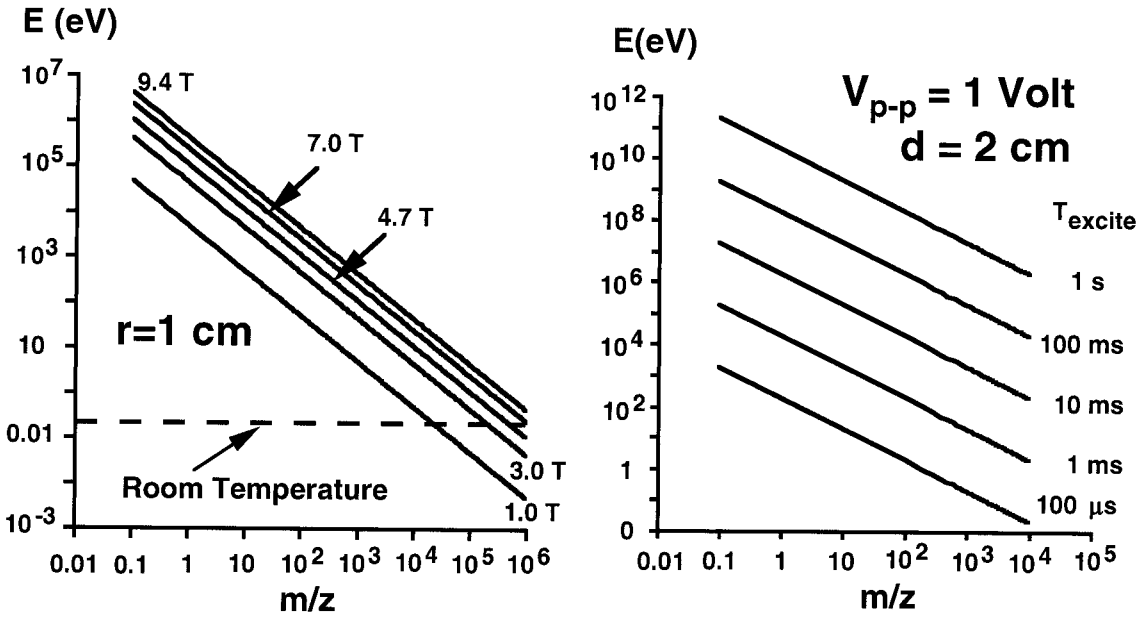

FIGURE 8. Post-excitation ion kinetic energy as a function of ion mass. Left: Fixed post-excitation cyclotron radius of 1 cm, for each of five magnetic field strengths: 1.0, 3.0, 4.7, 7.0, and 9.4 tesla. Right: Fixed excitation electric field = 1 $V_{p\text{-}p}$ applied between electrodes 2 cm apart, for each of five excitation durations.

to induce a detectable signal, even if all ions of a given mass-to-charge ratio had the same cyclotron phase. Thus, resonant excitation, as just described above, creates *spatial coherence* (and thus a detectable signal) from an ion packet whose cyclotron orbits are (say) initially centered on the *z*-axis, by increasing the ion cyclotron radius moving the ion initial packet significantly *off-axis* (see Fig. 5, left).

The difference, ΔQ, in ''image'' charge on two opposed infinitely extended parallel flat conductive plates, induced by an ion of charge, q, between the plates, is given by (see Fig. 6).

$$\Delta Q = -\frac{2qy}{d}. \tag{15}$$

The ICR signal is proportional to the induced current, $d\Delta Q/dt = -2q(dy/dt)/d$ (Comisarow, 1978; Guan and Marshall, 1995; Limbach et al., 1993), and is thus *independent of magnetic field strength.* Moreover, because the ion *y*-velocity component, dy/dt, increases linearly with ion cyclotron radius [Eq. (5)], the ICR signal increases *linearly* with ion cyclotron post-excitation radius. Moreover, the detected signal increases linearly with ion charge, so that ICR is increasingly more sensitive for multiply charged ions (as from electrospray ionization). Linearity is especially important for two reasons. First, because the ICR signal varies linearly with ion cyclotron post-excitation radius (which in turn depends linearly on the excitation voltage amplitude-duration product), the ICR response at *any* frequency is proportional to the excitation spectral magnitude at that frequency. (We'll use that idea in the next section to show how frequency-sweep or off-resonant or SWIFT excitation works.) Second, a Fourier transform of the time-domain ICR response gives the same ''absorption'' spectrum that would otherwise have been obtained by measuring power absorption while sweeping infinitely slowly across the *m*/*z* range (Marshall and Verdun, 1990). In addition, the ''superposition'' principle implies that the signals from any number of ions of arbitrary *m*/*z* values simply add at the detector; thus, ions of a wide *m*/*z* range can be detected *simultaneously.* The previous two statements combine to constitute the ''multichannel'' advantage of pulsed excitation followed by Fourier transformation to yield a spectrum of N data points in 1/N the time it would take to scan the spectrum one channel at a time (Marshall and Verdun, 1990). We shall next examine broadband excitation and defer further consideration of the ICR signal until we have discussed the effect of ion-neutral collisions.

C. Broadband Excitation

So far, we have examined the response of an ion in a static spatially homogeneous magnetic field, $\mathbf{B} = -B_0\mathbf{k}$, to a single-frequency resonant (at ω_c) oscillating electric field, $\boldsymbol{E}(t) = E_0\cos\,\omega_c t\mathbf{j}$. However, the very act of turning the

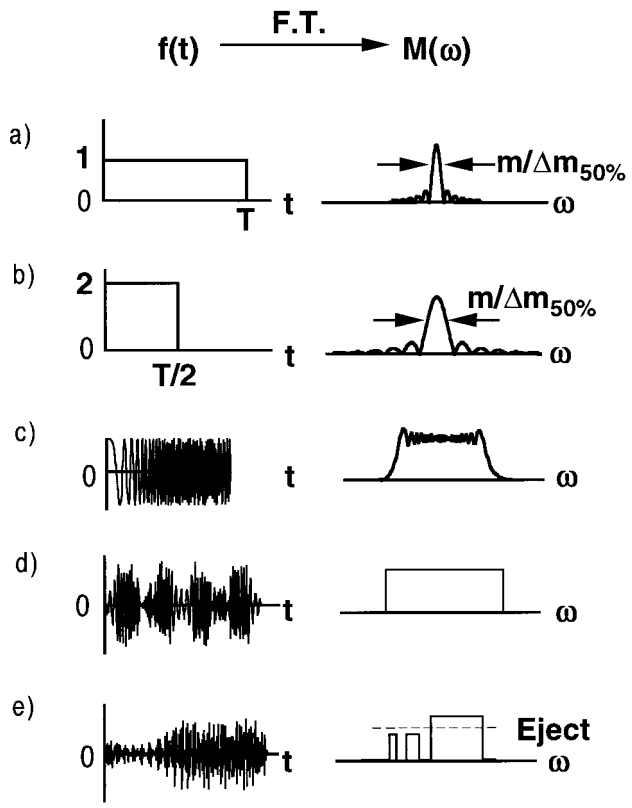

FIGURE 9. Time-domain (left) and frequency-domain (right) excitation waveforms. (a), (b) Rectangular pulses. (c) Frequency-sweep (''chirp''). (d), (e) Stored waveform inverse Fourier transform (''SWIFT'') waveforms.

excitation on and off generates excitation at other frequencies, as shown in Fig. 9(a). For example, the frequency-domain spectrum, $E(\nu)$, of single-frequency excitation at frequency, $\omega_c = 2\pi\nu_c$, applied steadily for $T_{\text{excit'n}}$ seconds, is given by (Marshall and Verdun, 1990).

$$E(\nu) = E_0 \frac{\sin(2\pi\nu_c T_{\text{excit'n}})}{2\pi\nu_c} . \qquad (16)$$

Thus, although the applied excitation may be precisely centered at a frequency, ω, which differs from ω_c, turning the excitation voltage on at time zero and off at time, $T_{\text{excit'n}}$, effectively broadens the spectral range of the excitation (to a bandwidth of $\sim 1/T_{\text{excit'n}}$ rad s^{-1}). The longer the time-domain signal duration, the narrower is its corresponding frequency-domain spectral width. Thus, if an *off-resonance* excitation at frequency, υ, is sufficiently brief so that $(1/T_{\text{excit'n}}) \geq 2\pi|\nu - \nu_c|$, it can still excite ions of cyclotron frequency, ω_c. This general result defines the ultimate precision with which ions can be mass-selected by their ICR frequencies. Fortunately, because ion cyclotron frequencies are so high (typically kHz to MHz), excitation for as short as one second is still exquisitely mass-selective (e.g., $\sim$10 ppm for ions of m/z 1000 at 7.0 tesla).

Equation (16) shows that a single-frequency excitation of duration, $T_{\text{excit'n}}$, can excite ions whose ion cyclotron frequencies span a range of $\sim 0.1/T_{\text{excit'n}}$ Hz to near-uniform cyclotron radii. (Because ICR signal magnitude is proportional to post-excitation ICR orbital radius, which is in turn proportional to excitation magnitude, we seek a flat excitation magnitude spectrum in order to produce a mass spectrum whose peak areas accurately reflect the relative abundances of ions of different m/z.) However, Figure 9(a),(b) shows that doubling the excitation frequency-domain bandwidth while maintaining the frequency-domain magnitude requires halving the time-domain excitation duration and doubling the time-domain amplitude. Thus, given that a single-frequency resonant excitation voltage of ± 1 volt (between electrodes $\sim$2 cm apart) is needed to excite ions to a detectable cyclotron radius of 1 cm in 1.4 ms [based on Eq. (13)], the excitation of ions anywhere within a bandwidth $\sim$1 MHz to near-uniform cyclotron radii will require a single-frequency excitation of ~ 0.1 μs [i.e., $\sim$1/10 of the width of the ''sinc'' function of Eq. (10)], which corresponds to $\sim \pm$10,000 volt (i.e., inconveniently large) rf excitation voltage. Therefore, broadband ion cyclotron excitation is commonly performed by frequency-sweep (''chirp'') excitation [Fig. 9(c)] (Comisarow and Marshall, 1974; Marshall and Roe, 1980; Marshall and Verdun, 1990), which achieves the excitation of a relatively flat magnitude over a broad frequency range by use of a relatively low excitation voltage (see Section VII).

The disadvantages of chirp excitation are evident in Fig. 9(c): nonuniform excitation amplitude (translating to variation in apparent ion relative abundances) across the spectrum, and limited mass selectivity at the start and end frequencies of the sweep. Fortunately, a very general excitation mode is made possible by the highly linear excitation/response of ICR. The idea is simply to reverse the process, and begin by defining the desired excitation profile in the mass-domain, converting it to a frequency-domain excitation spectrum, and performing an *inverse* Fourier transform to generate the desired time-domain excitation waveform (Marshall et al., 1988; Marshall et al., 1985), as shown in Figs. 9(d),(e). In this way, one can create mass spectral ''windows'' within which none (or all) of the ions are excited or ejected, thereby providing complete broadband mass selectivity for MS/MS or for enhanced dynamic range (Wang et al., 1986) by selective ejection of highly abundant ions. SWIFT achieves the flattest and most frequency-selective excitation magnitude spectrum theoretically possible for a given time-domain excitation period. The principles and uses for SWIFT excitation [for both Penning (ICR) and Paul (quadrupole)] ion

traps have recently been reviewed (Guan and Marshall, 1996).

D. Broadband Detection; Detection Limit

A coherently orbiting ion packet induces a differential current between two opposed detection plates and may be modeled as a current source. The receiver plates and wiring that connect the ion trap to the detection preamplifier have an inherent resistance and capacitance in parallel (see Fig. 7) (Comisarow, 1978; Limbach et al., 1993). Experimentally, at typical ICR frequencies (>10 kHz) the signal-to-noise ratio is independent of cyclotron frequency. However, at sufficiently low frequency (<10 kHz), the signal varies directly with frequency. Therefore, throughout most of the frequency range excited by a broadband chirp or SWIFT waveform in a standard FT-ICR MS experiment, the detected signal-to-noise ratio reflects the relative current differential induced on the detection plates. Furthermore, the detection limit (namely, the minimum number, N, of ions that may be detected from an undamped signal in a single 1-s acquisition period to yield a S/N ratio of 3:1) may be calculated from the following equation:

$$N = \frac{CV_{d(p\text{-}p)}}{qA_1(r)}, \tag{17}$$

in which C is the capacitance of the detection circuit, $V_{dp\text{-}p}$ is the peak-to-peak amplitude of the detected voltage (calibrated for a given spectrometer), and $A_1(r)$ is a coefficient that is approximately proportional to r and may be determined graphically (Grosshans and Marshall, 1990). For example, for typical operating parameters, namely, a detection circuit capacitance of 50 pF, $V_{d(p\text{-}p)}$ of 3×10^{-7} V, and $A_1(r) = 0.5$ (i.e., the ion is excited to approximately half of its maximal cyclotron radius), an observed signal-to-noise ratio of 3:1 corresponds to a detection limit of ~187 ions.

IV. ION-NEUTRAL COLLISIONS

For ions of a single m/z value, the ICR frequency-domain response in the absence of collisions looks just like Eq. (16), and is obtained by Fourier transformation of a digitized time-domain signal to give a ''sinc'' function spectrum that looks just like Eq. (9a), except that $T_{\text{excit'n}}$ is replaced by the data acquisition period, $T_{\text{acq'n}}$. The simplest way to treat ion-neutral collisions is to model their effect as a frictional damping force in the overall ion equation of motion:

$$\text{Force} = m\frac{d\boldsymbol{v}}{dt} = q\boldsymbol{E} + q\boldsymbol{v} \times \boldsymbol{B} - f\boldsymbol{v}. \tag{18}$$

This model (Beauchamp, 1967; Wobschall et al., 1963) leads to an exponential damping of the time-domain ICR signal for N_i ions of ICR frequency, ν_i,

$$s_i(t) \propto N_i \exp(-t/\tau_i)\cos(2\pi\nu_i t), \tag{19}$$

whose Fourier transform yields a Lorentzian frequency-domain magnitude-mode spectrum.

$$M(\omega) \propto \frac{\tau}{\sqrt{1 + (\omega - 2\pi\nu_i)^2\tau^2}}. \tag{20}$$

Thus (see Fig. 10), FT-ICR spectral line shape approaches the ''sinc'' shape in the limit of zero pressure (i.e., $\tau \gg T_{\text{acq'n}}$, so that there are essentially no ion-neutral collisions during data acquisition), and approaches the Lorentzian shape in the ''high-pressure'' limit ($\tau \ll T_{\text{acq'n}}$) that the signal has damped nearly to zero during the data acquisition period. These line shapes define mass resolution and mass resolving power, as discussed below. τ may be defined as follows (Wobschall et al., 1963):

$$\frac{1}{\tau} = \frac{m_{\text{neutral}}}{m_{\text{ion}} + m_{\text{neutral}}}\nu_{\text{collision}}, \tag{21}$$

in which $\nu_{\text{collision}}$ is the number of ion–molecule collisions per second. In order to calculate $\nu_{\text{collision}}$, one must first determine the rate constant for ion–molecule collisions. At thermal velocity, an ion and a neutral molecule interact through the ion-induced dipole (''Langevin'') potential (Steinfeld et al., 1989):

$$U(r) = -\frac{\alpha' q^2}{8\pi\varepsilon_0 r^4} \quad \text{(S.I. units)} \tag{22a}$$

$$U(r) = -\frac{\alpha' q^2}{2r^4} \quad \text{(cgs units)}, \tag{22b}$$

in which q is the ion charge, α' is the isotropic polarizability of the neutral, r is the distance between the two bodies, and the ion is modeled as a point charge. From this interaction potential and the Langevin model, the ion-neutral collision rate constant may be calculated:

$$k = \sqrt{\frac{\pi\alpha' q^2}{\varepsilon_0\mu}} \quad \text{(S.I. units)} \tag{23a}$$

$$k = \sqrt{\frac{4\pi^2\alpha' q^2}{\mu}} \quad \text{(cgs units)}. \tag{23b}$$

At this juncture, a note about units is in order. k is

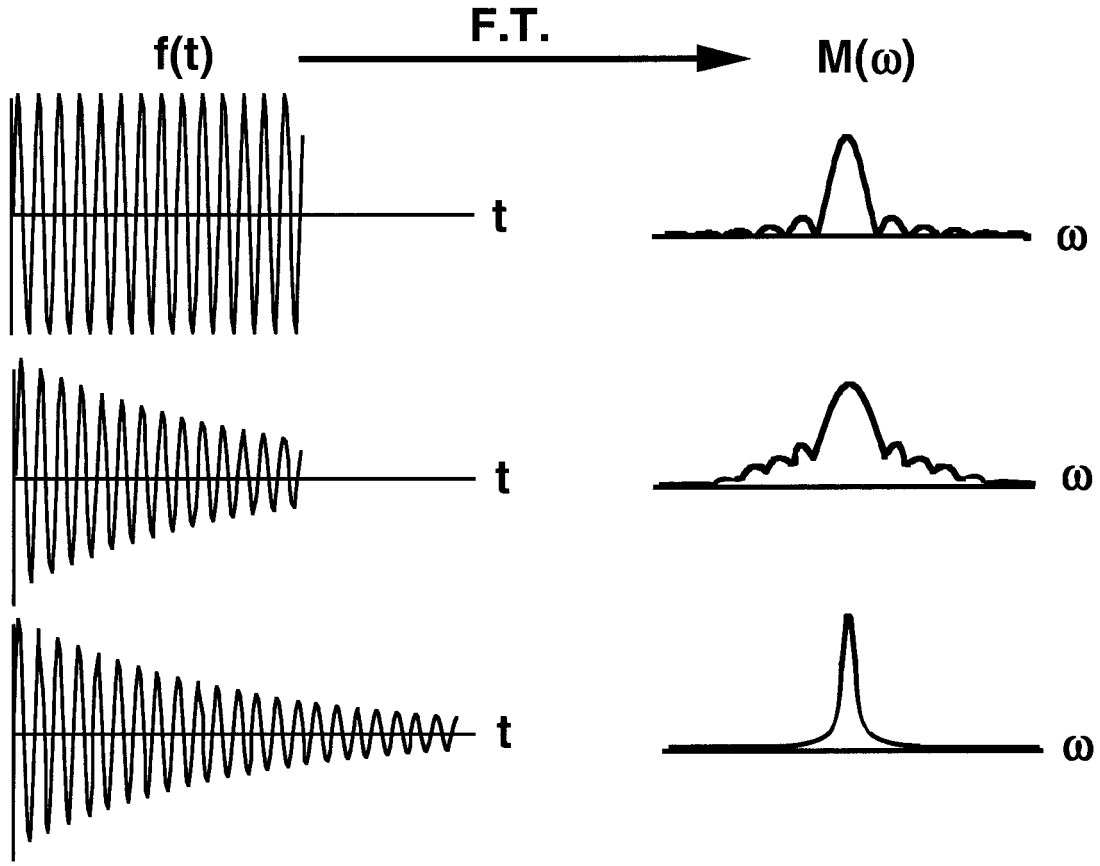

FIGURE 10. Simulated time-domain ICR signals (left) and frequency-domain magnitude spectra (right) for low-pressure, $\tau \gg T_{acq'n}$ (top), intermediate-pressure, $\tau \approx T_{acq'n}$ (middle), and high-pressure, $\tau \ll T_{acq'n}$ (bottom) limits.

almost always reported in cgs units. In cgs units, the elementary charge, q, is 4.80653×10^{-10} statcoulombs (electrostatic units or esu); α' is in cm^3; and μ (the reduced mass of the ion and molecule) is in grams. Thus, in order to obtain the collision frequency for one ion, pressure must be computed as the number of molecules per cm^3. For example, suppose that the pressure inside the Penning trap is 1×10^{-8} torr, corresponding ($PV = nRT$) to a neutral concentration of 3.24×10^8 molecules/cm^3 at a temperature of 298.15 K. For an ion of 100 u colliding with nitrogen (N_2) molecules, the neutral polarizability, α', equals 1.7403×10^{-24} cm^3 (Weast, 1989–1990). From these values, Eq. (23) yields an ion-neutral collision rate constant, $k = 6.61 \times 10^{-10}$ cm^3 s^{-1}. If we now multiply this number by the neutral concentration, then we obtain $\nu_{collision} \approx 0.2$ collisions per second per ion.

Recently, it has been pointed out that the collisional model just described derives from a Langevin (ion/induced-dipole) collision model (Langevin, 1905). Although the Langevin model offers a good description for room-temperature ions, a hard-sphere collision model is much more appropriate for the much higher velocities of ions during FT-ICR data acquisition. Equations (17) and (18) take the form (Guan et al., 1998)

$$\text{Force} = m\frac{dv}{dt} = q\boldsymbol{E} + qv \times \boldsymbol{B} - fv^2. \tag{24}$$

Instead of an exponential damping of the ion velocity with time, the ion velocity, $v(t)$, is now represented by

$$v(t) = \frac{v_0}{1 + v_0(m_{neutral}/(m_{neutral} + m_{ion}))N\sigma_{Hard\ Sphere}t}, \tag{25}$$

in which N is the neutral number density, $\sigma_{Hard\ Sphere}$ is the hard-sphere collision cross-section, and $m_{neutral}$ and m_{ion} are the neutral and ion masses, respectively. Although there is no analytical Fourier transform of Eq. (21), it can be transformed numerically to yield a frequency-domain line shape that has a narrow width at half-maximum peak height, but is very broad at the base. At present, FT-ICR time-domain signals are typically weighted (''windowed'', ''apodized'') to suppress the broad base of the ''true'' hard-sphere line shape; however, the natural line shape

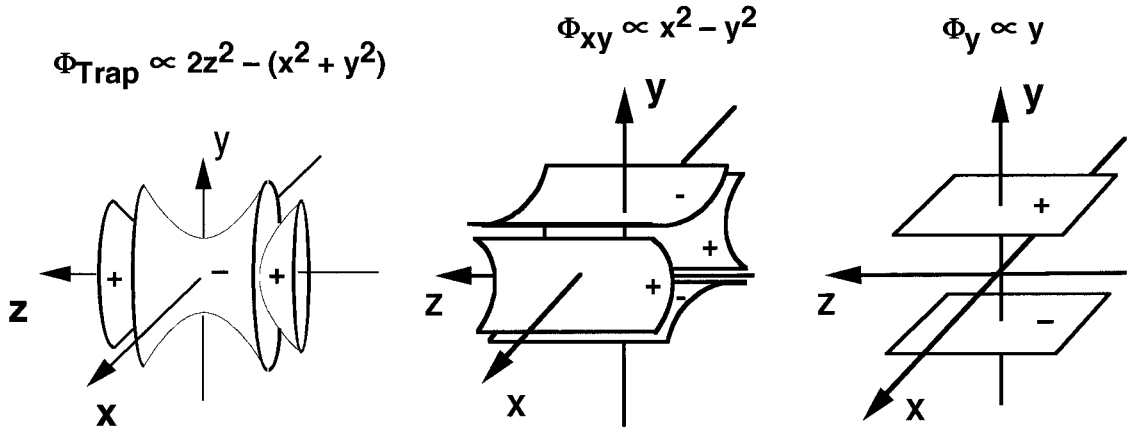

FIGURE 11. Plot of isopotential surfaces for trapping (left), 2D quadrupolar (middle), and dipolar (right) potentials.

may prove useful for future quantitation of ion-neutral collision frequencies (e.g., for comparison to ion mobilities measured in beam instruments).

V. EFFECTS OF AXIAL CONFINEMENT OF IONS IN A TRAP OF FINITE SIZE

Up to now, we have considered only idealized ion behavior in a spatially uniform **B** field and an orthogonal spatially uniform oscillating **E** field. Here we show how those results are modified by the need to perform the experiment in a ''cell'' of finite dimensions. First, a static magnetic field applied along the *z*-direction effectively confines ions in the *x*- and *y*-directions, according to the cyclotron motion described above. However, ions are still free to escape along the *z*-axis (i.e., along or opposed to the magnetic field direction). In order to prevent such an escape, it is usual to apply a small (~1 volt) electrostatic potential (ideally three-dimensional axial quadrupolar—see below) to each of two ''end cap'' electrodes that are positioned at $z = \pm a/2$ from the center of the ''cell.'' Second, because the electrodes that generate the electrostatic trapping potential and the excitation (or detection) electric potentials are necessarily finite in size, the resultant electric field is nonlinear (and reduced in magnitude) from that from infinitely extended opposed parallel flat conductive plates. We next show briefly how these two perturbations affect the FT-ICR experiment.

A. Axial Ion Oscillation Due to a *z*-Component of Electrostatic Trapping Potential

The optimal one-dimensional potential for axial confinement of ions would be a simple quadratic potential, $\Phi(z) \propto (z^2/2)$, because the gradient of that potential yields a simple harmonic restoring force, so that ions oscillate sinusoidally back and forth between the end cap electrodes at a frequency independent of ion *z*-position. However, in three dimensions, Laplace's equation, $\nabla^2\Phi(x, y, z) = 0$, requires the addition of terms in x^2 and y^2. Hans Dehmelt and Wolfgang Paul, in work that laid the basis for their shared Nobel prize in 1989, exploited the experimentally convenient (i.e., cylindrically symmetric) three-dimensional axial quadrupolar electrostatic trapping potential of the form

$$\Phi(x, y, z) = V_{trap}\left(\gamma + \frac{\alpha}{2a^2}(2z^2 - x^2 - y^2)\right) \qquad (26a)$$

or

$$\Phi(r, z) = V_{trap}\left(\gamma + \frac{\alpha}{2a^2}(2z^2 - r^2)\right), \qquad (26b)$$

in which $r = \sqrt{x^2 + y^2}$ is the radial position of the ion in the *x*-*y* plane, *a* is a measure of trap size, and γ and α are constants that depend on the trap shape (Dehmelt, 1990). The shape of the potential of Eq. (26) is graphically evident from a plot of its isopotential surfaces (Fig. 11).

Values of γ and α for several ICR trap shapes (Fig. 12) in common use are shown in Table 1. The methodology for computing γ and α for orthorhombic, tetragonal, and cylindrical traps of arbitrary aspect ratio is available (Jackson et al., 1997). The dipolar excitation fields for cubic and cylindrical (unit aspect ratio) traps are essentially identical, if the excitation voltage is ~1.4 times higher for the cylindrical trap; similarly, the detected signal from the cylindrical trap is ~0.7 of that for a cubic trap

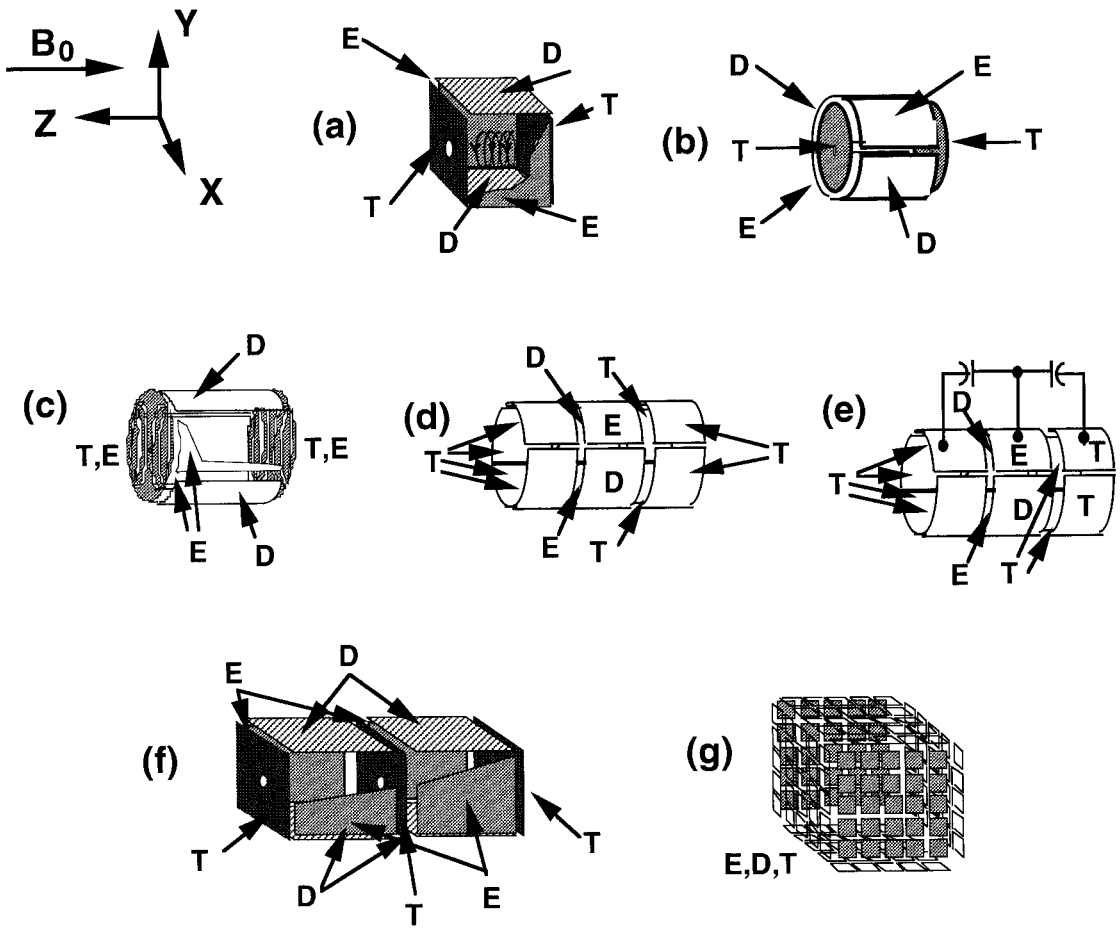

FIGURE 12. ICR ion trap configurations. E = Excitation; D = Detection; T = End Cap (''Trapping''). (a) cubic (Comisarow, 1981; Comisarow, 1980); (b) cylindrical (Comisarow and Marshall, 1976; Elkind et al., 1988; Kofel et al., 1986; Lee et al., 1980); (c) end caps segmented to linearize excitation potential (''infinity'' trap) (Caravatti and Allemann, 1991); (d) and (e) open-ended, without or with capacitive rf coupling between the three sections (Beu and Laude, 1992; Beu and Laude, 1992; Gabrielse et al., 1989); (f) dual (Littlejohn and Ghaderi, 1986); and (g) ''matrix-shimmed'' (Guan and Marshall, 1995).

whose corners just touch the inner walls of the comparable cylindrical trap. [We have chosen a cubic trap inscribed (rather than circumscribed) relative to a cylinder, because both traps each have the largest possible equal diameter, and thus are equally separated from the inner (cylindrical) wall of the enveloping vacuum chamber.] The hyperbolic trap is near-perfect for trapping potential, but is very nonlinear for dipolar excitation. Although capacitive coupling of the three-cylinder open trap improves its dipolar excitation linearity only slightly for ions in the $z = 0$ midplane, the capacitively coupled design provides near-linear excitation from one end of the trap to the other, and, therefore, virtually eliminates ''*z*-ejection.'' Also, although β_{quad} for the matrix-shimmed trap is not as large as for the cylindrical traps, it closely approximates the ''ideal'' β_{quad} of 8/3 (i.e., the limiting value for an infinitely extended tetragonal trap). The ''infinity'' trap improves dipolar excitation, but not (in the absence of an additional switching network) dipolar detection, and requires that quadrupolar excitation be performed with 2-plate rather than 4-plate excitation (Jackson et al., 1997).

From Eq. (26), it is straightforward to solve the equation of ion *z*-motion

$$\text{Axial Force} = m\frac{d^2z}{dt^2} = -q\nabla\Phi(x, y, z) \tag{27}$$

to obtain an ion *z*-position that oscillates sinusoidally with time,

$$z(t) = z(0)\cos(2\pi\nu_z t) \tag{28a}$$

$$\nu_z = \frac{1}{2\pi}\sqrt{\frac{2qV_{\text{trap}}\alpha}{ma^2}} \quad \text{(S.I. units)} \tag{28b}$$

TABLE 1. Trapping [γ, α in Eq. (26)], azimuthal dipolar excitation [β_{dipolar}, Eq. (34)] and two-dimensional azimuthal quadrupolar excitation [β_{quad}, Eq. (36)] scale factors for trap shapes in common use in FT-ICR MS.

Trap shape	End cap separation	Excitation electrode separation	γ	α	β_{dipolar}	β_{quad}
Ideal	NA	NA	0.50000	4.00000	1.00000	2.66667
Cube[a]	a	$d = a$	0.33333	2.77373	0.72167	2.77373
Cylinder[b]	a	d	0.2787	2.8404	0.80818	3.25522
Infinity	a	d	0.2787	2.8404	$\approx$0.900[c]	NA[d]
Open uncoupled[e]	a	d	0.14527	3.86798	0.86738	3.30527
Open coupled[e]	a	d	0.14527	3.86798	0.89699	3.34800[f]
Hyperbolic[g]	a	$d = \sqrt{2}\,a$	0.44403	4.0905	0.66483	2.6469
Matrix-shimmed cube	a	d	0.50000	3.9254	$\approx$1[h]	2.6264

[a] (Rempel et al., 1986).
[b] Unit aspect ratio (Kofel et al., 1986; Mitchell et al., 1994).
[c] Approaches the value of β_{dipolar} for an infinitely long cylindrical trap.
[d] Cannot perform ''traditional'' 4-plate quadrupolar excitation without additional circuitry and switching; however, 2-plate quadrupolar excitation may be used instead.
(Hendrickson et al., 1995).
[e] Three consecutive right circular cylinders, each of unit aspect ratio, capacitively coupled or not. In this case, a refers to the length of the central cylinder.
[f] Requires capacitive coupling of the detection electrodes as well as the excitation electrodes.
[g] (Knight, 1983; Yin et al., 1992).
[h] Up to a radius of $a/4$ (i.e., halfway from the trap central axis to the side of the trap).

$$\boxed{\nu_z = 2.21088 \times 10^3 \sqrt{\frac{zV_{\text{trap}}\alpha}{ma^2}}}$$

$$\left(\begin{array}{l}\nu_z \text{ in Hz; } V_{\text{trap}} \text{ in volts; } a \text{ in m; } m \text{ in u;}\\ z \text{ in multiples of elementary charge}\end{array}\right). \quad (28c)$$

For example, for $V_{\text{trap}} = 1$ volt in a cubic trap of side length, $a = 2.54$ cm, an ion of $m/z = 1000$ will oscillate at a ''trapping'' frequency of 4,580 Hz.

B. Radial Ion "Magnetron" Rotation Due to a Combination of B-Field and r-Component of Electrostatic Trapping Potential

The d.c. ''trapping'' potential of Eq. (26) also produces a radial force:

$$\text{Radial Force} = qE(r) = \frac{qV_{\text{trap}}\alpha}{a^2}\,r. \quad (29)$$

The radial electric field that acts on the ion produces an outward-directed electric force that opposes (and, thus, has opposite sign with respect to) the *inward*-directed Lorentz magnetic force from the applied magnetic field. We can now combine Eq. (29) with Eq. (4a) to obtain the equation for ion motion subject to a static $\mathbf{B} = -B_0\mathbf{k}$ field *and* a three-dimensional axial quadrupolar electrostatic potential of Eq. (19b):

$$\text{Force} = m\omega^2 r = qB_0\omega r - \frac{qV_{\text{trap}}\alpha}{a^2}\,r \quad (30a)$$

or

$$\omega^2 - \frac{qB_0\omega}{m} + \frac{qV_{\text{trap}}\alpha}{ma^2} = 0. \quad (30b)$$

Note that Eq. (30b) is a quadratic equation in ω, but that ω is *independent of r*! That is the great advantage of the three-dimensional axial quadrupolar d.c. trapping potential—namely, each resultant ion motional frequency (see below) is independent of ion position inside the trap. Solving Eq. (30b) for ω, we obtain *two* natural rotational frequencies (in rad s^{-1}) in place of the original ''unperturbed'' cyclotron frequency that is observed in the absence of a d.c. trapping potential.

$$\omega_+ = \frac{\omega_c}{2} + \sqrt{\left(\frac{\omega_c}{2}\right)^2 - \frac{\omega_z^2}{2}} \quad \text{(''Reduced'' cyclotron frequency)} \quad (31a)$$

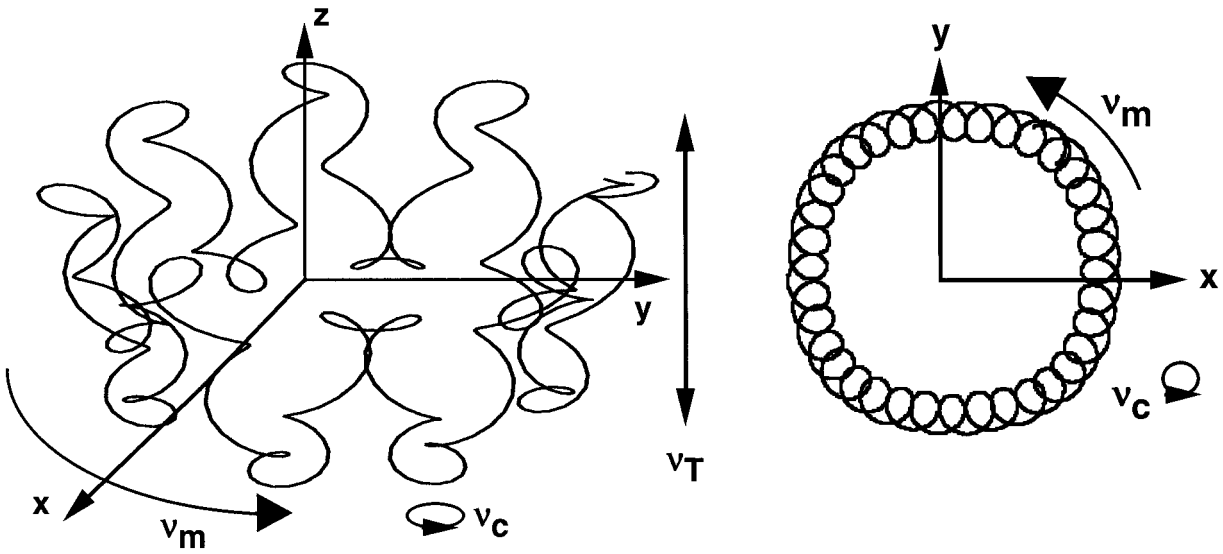

FIGURE 13. Ion motion in a 2 in. cubic Penning trap in a perfectly homogeneous magnetic field of 3T for an ion of *m*/*z* 2,300, for 10V trapping voltage. The three natural motional frequencies and amplitudes have relative magnitudes given by: $\omega_+ = 4.25\ \omega_z$, $\omega_z = 8.5\ \omega_-$, $\rho_- = 4z_{max} = 8\rho_+$ (Schweikhard et al., 1995). Note that the field produced by a cubic trap is not perfectly quadrupolar as manifested by the shape of the magnetron orbit (not a perfect circle) in the *xy* plane. The magnetic field points in the negative *z* direction.

$$\omega_- = \frac{\omega_c}{2} - \sqrt{\left(\frac{\omega_c}{2}\right)^2 - \frac{\omega_z^2}{2}} \quad (\text{''Magnetron'' frequency}) \qquad (31b)$$

in which

$$\omega_z = \sqrt{\frac{2qV_{trap}\alpha}{ma^2}}$$

(''Trapping'' oscillation frequency, in S.I. units) (31c)

and

$$\omega_c = \frac{qB_0}{m} \quad (\text{''Unperturbed'' cyclotron frequency, S.I. units}). \qquad (4a)$$

The three natural ion motional modes (cyclotron rotation, magnetron rotation, and trapping oscillation) are shown in Fig. 13, and their relative frequencies as a function of ion *m*/*z* and d.c. trapping potential are shown in Fig. 14 (Schweikhard et al., 1995). The magnetron and trapping frequencies are usually much less than the cyclotron frequency, and generally are not detected (except as small sidebands when the ion trap is misaligned with the magnet axis and/or the ion motional amplitudes approach the dimensions of the trap) (Allemann et al., 1981; Marshall and Grosshans, 1991; Mitchell et al., 1989).

C. Mass Calibration

Equation (31a) shows that the imposition of a quadrupolar d.c. trapping potential *reduces* the ion cyclotron orbital frequency, because the radially outward-directed magnetic field effectively reduces the magnetic field strength. In the absence of electric space charge and trapping potentials, measurement of the frequency of a *single* ion of known mass would serve to calibrate the magnetic field strength, from which the *m*/*z* values of all other ions in the mass spectrum could be computed from Eq. (4a). However, the introduction of a trapping potential changes the ICR mass/frequency relation to the form shown in Eq. (31a), from which Eq. (32) can be derived (Ledford et al., 1984). *A* and *B* are constants obtained by fitting a particular set of ICR mass spectral peak frequencies for ions of at least two known *m*/*z* values to Eq. (32).

$$\frac{m}{z} = \frac{A}{\nu_+} + \frac{B}{\nu_+^2}\,. \qquad (32)$$

Strictly speaking, Eqs. (31) and (32) should be valid only in the single-ion limit (i.e., no Coulomb interactions between ions). In practice, however, FT-ICR MS experiments are usually performed with sufficiently few ions so that the space charge perturbation is small; moreover, the perturbation affects calibrant and analyte ions. That's basically why ICR mass calibration works so well, even when many ions are present. ''Internal'' calibration (i.e., cali-

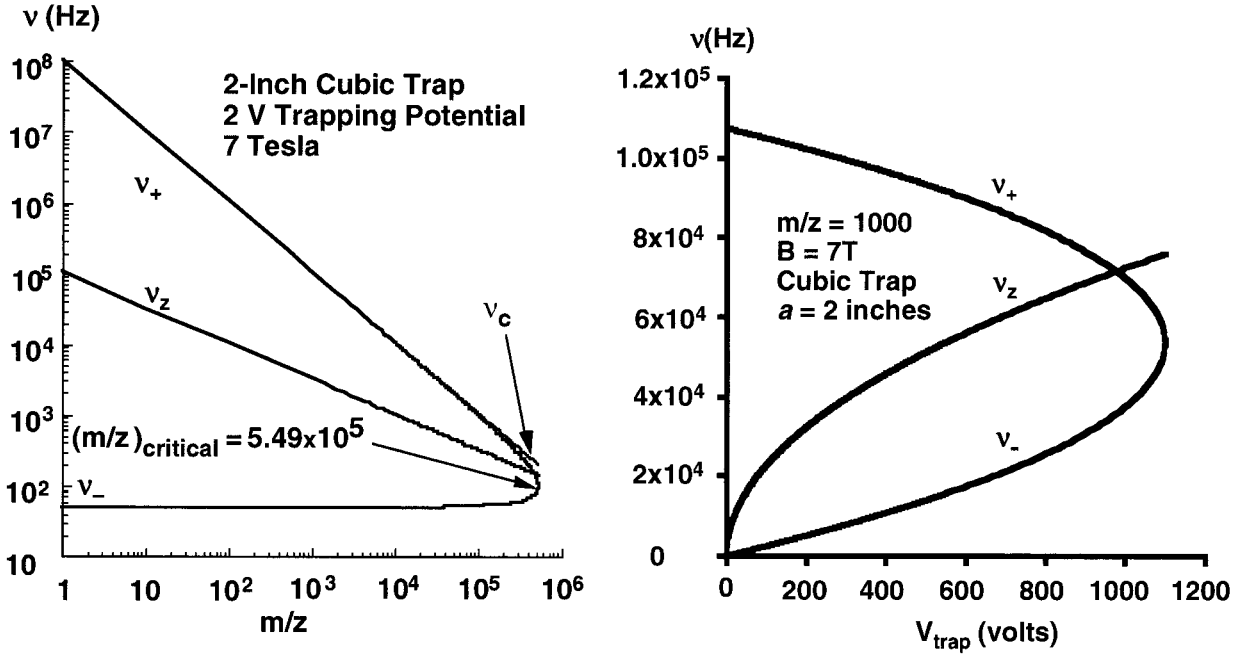

FIGURE 14. Left: Mass-to-charge ratio (m/z) dependence of the frequency of each of the three ion natural motions (cyclotron rotation, magnetron rotation, and axial oscillation) in an ICR (Penning) ion trap [see Eq. (31)]. At m/z values well below the ''critical'' m/z, the reduced cyclotron frequency, ν_+, is approximately inversely proportional to m/z, whereas axial frequency, ν_z, is approximately inversely proportional to the square root of m/z, and magnetron frequency is nearly independent of m/z. At the ''critical'' m/z value, $\nu_+ = \nu_- = \nu_z/\sqrt{2} = \nu_c/2$ [see Eq. (40)]. At or above the ''critical'' m/z value, ions are no longer trapped. (Reproduced, with permission, from (Guan and Marshall, 1996).) Right: Natural motional frequencies as a function of d.c. trapping potential. Note the maximum trapping potential above which ions are not confined radially.

brant ions are present along with analyte ions in the same sample) typically improves mass accuracy by a factor of at least 3 compared to ''external'' calibration (i.e., calibration is performed on a separate sample from the analyte). External calibration works best when calibrant ions are excited to the same cyclotron radius as analyte ions, and when the number of ions in the trap is the same for both experiments.

VI. QUADRUPOLAR EXCITATION, AXIALIZATION, AND ION REMEASUREMENT

So far, we have shown that a three-dimensional axial quadrupolar electrostatic potential (Fig. 11, left) is optimal for *trapping* ions for ICR, and that a one-dimensional *linear* rf electric potential (Fig. 11, right), which produces a spatially uniform rf electric field, is optimal for ICR excitation/detection. We now discuss the purpose of a two-dimensional azimuthal quadrupolar rf potential (Fig. 11, middle). It can be shown (Bollen et al., 1990) that such a potential (oscillating at the unperturbed ion cyclotron frequency, $\omega_c = qB_0/m$) periodically interconverts magnetron and cyclotron motions. As a matter of fact, it has been shown that such an experiment is formally analogous to resonant excitation in a two-level spin one-half magnetic resonance experiment: conversion from pure magnetron to pure cyclotron motion corresponds to population inversion by a π-pulse (Guan, 1992).

In the presence of collisions, ion magnetron radius increases slowly with time, whereas ion cyclotron radius decreases rapidly with time. Thus, if magnetron radius (i.e., the radial position of the center of an ion cyclotron orbit) is converted to cyclotron radius (by two-dimensional azimuthal quadrupolar excitation at frequency, ω_c), then collisions will rapidly damp the cyclotron motion to zero, and ions will relax toward the central axis of the ion trap. The interconversion frequency is given by (Guan et al., 1994)

$$\omega_{\text{interconvert}} = \frac{3(2.66667)qV_{\text{quad}}}{2md^2(\omega_+ - \omega_-)} \quad \text{(S.I. units)} \qquad (33a)$$

or

$$\nu_{\text{interconvert}} = \frac{9.77601 \times 10^6 z V_{\text{quad}}}{m d^2 (\nu_+ - \nu_-)}$$

$$\left(\begin{array}{c} \text{Frequencies in Hz; } V_{\text{quad}} \text{ in volts; } d \text{ in m; } m \text{ in u;} \\ z \text{ in multiples of elementary charge} \end{array} \right), \quad (33b)$$

in which $\pm V_{\text{quad}}$ is the voltage applied to electrodes separated by d m, and 2.66667 is an ideal scaling factor that corresponds to an infinitely extended tetragonal trap (β_{quad}, see next section), in the configuration shown in Fig. 11 (middle). For example, for ions of m/z 1000, the application of two-dimensional azimuthal quadrupolar excitation of ± 1 volt amplitude to electrodes separated by 2.54 cm in the configuration of Fig. 11 (middle), at the unperturbed ion cyclotron frequency (107,500 Hz at 7.0 tesla), will interconvert magnetron and cyclotron motion at a frequency of ~141 Hz. Thus, if those ions have zero initial cyclotron radius at time, zero, then their magnetron motion will be completely converted to cyclotron motion in ($\frac{1}{2}\nu_{\text{interconvert}}$), or ~3.5 ms.

The conversion of magnetron motion to cyclotron motion, followed by collisional damping of the cyclotron radius, has come to be known as quadrupolar axialization (Guan et al., 1994). By ''shrink-wrapping'' a packet of ions that was initially distributed widely in radius (e.g., as a result of ion initial formation or injection into the ion trap), axialization improves virtually every aspect of FT-ICR performance: mass resolving power and mass accuracy; cooling of ion internal energy; mass selectivity for MS^n; collision-induced dissociation efficiency; transfer efficiency in dual-trap experiments; and ion remeasurement efficiency. Ion remeasurement (Speir et al., 1993; Williams et al., 1990) is especially useful for improving the signal-to-noise ratio (and improving the ICR detection limit) (Solouki et al., 1995) and for high-resolution MS^n (Solouki et al., 1996). Finally, quadrupolar axialization combined with nondestructive ICR detection enhances user-interactive FT-ICR MS (Guan and Marshall, 1997).

VII. EFFECT OF TRAP SIZE AND SHAPE ON DIPOLAR AND TWO-DIMENSIONAL QUADRUPOLAR EXCITATION

Equations (13) and (14) give the ion cyclotron radius, r, and translational energy, K.E., after single-frequency resonant azimuthal dipolar excitation by a spatially uniform rf electric field. To a good approximation, those equations also apply for similar excitation in a finite-size ion trap by inclusion of a scaling factor, β.

$$r = \frac{\beta_{\text{dipolar}} E_0 T_{\text{excite}}}{2B_0} \quad (34a)$$

or

$$\boxed{r = \frac{\beta_{\text{dipolar}} V_{p-p} T_{\text{excite}}}{2dB_0}} \quad \text{(S.I. units)} \quad (34b)$$

or, for broadband frequency-sweep dipolar excitation,

$$\boxed{r = \frac{\beta_{\text{dipolar}} V_{p-p} \sqrt{\dfrac{1}{\text{Sweep Rate}}}}{2dB_0}} \quad (34c)$$

and

$$\text{K.E.}_{\text{post-excit'n}} = \frac{\beta^2_{\text{dipolar}} q^2 E_0^2 (T_{\text{excite}})^2}{8m} = \frac{\beta^2_{\text{dipolar}} q^2 V^2_{p-p} (T_{\text{excite}})^2}{8d^2 m} \text{ (S.I.)} \quad (35a)$$

$$\boxed{\text{K.E.}_{\text{post-excit'n}} = \frac{1.20607 \times 10^7 \beta^2_{\text{dipolar}} z^2 V^2_{p-p} (T_{\text{excite}})^2}{d^2 m}} \quad (35b)$$

$$\boxed{\text{K.E.}_{\text{post-excit'n}} = \frac{1.20607 \times 10^7 \beta^2_{\text{dipolar}} z^2 V^2_{p-p} \dfrac{1}{\text{Sweep Rate}}}{d^2 m}}, \quad (35c)$$

in which energy is in eV; V_{p-p} is in volts; $T_{\text{excit'n}}$ is in s; d is in m; m is in u; and z is in multiples of elementary charge. For example, for single-frequency resonant excitation at 10 V_{p-p} for 400 μs in a cubic Penning trap whose excitation plates are 2 cm apart, in a 7 T magnet field, the post-excitation cyclotron radius is 1.03 cm. Alternatively, ions having a wide range of mass-to-charge ratios may be excited to the same radius by frequency-sweep excitation (spanning the ICR frequencies of interest) of amplitude, V_{p-p} = 123 V, at a sweep rate of 1.00×10^9 Hz/s. It is worth noting that the magnitude mode spectral peak height is proportional to $1/\sqrt{\text{Sweep rate}}$.

Values of β_{dipolar} for several ICR traps in common use are shown in Table 1. A methodology for computing β_{dipolar} for orthorhombic, tetragonal, and cylindrical traps of arbitrary aspect ratio is available (Jackson et al., 1997).

Similarly, Eq. (33) for the interconversion frequency for azimuthal two-dimensional quadrupolar excitation is re-scaled as Eq. (36). Values of β_{quad} for several ICR traps in common use are shown in Table 1, and formulas for computing β_{quad} for orthorhombic, tetragonal, and cylindrical traps of arbitrary aspect ratio have been published (Jackson et al., 1997).

$$\omega_{\text{interconvert}} = \frac{3q\beta_{\text{quad}}V_{\text{quad}}}{2md^2(\omega_+ - \omega_-)} \quad \text{(S.I. units)} \tag{36a}$$

or

$$\nu_{\text{interconvert}} = \frac{2.30342 \times 10^7 z\beta_{\text{quad}}V_{\text{quad}}}{md^2(\nu_+ - \nu_-)}$$

$$\left(\begin{array}{c}\text{Frequencies in Hz; } V_{\text{quad}} \text{ in volts; } d \text{ in m; } m \text{ in u;} \\ z \text{ in multiples of elementary charge}\end{array}\right). \tag{36b}$$

Ideal scaling factors for all three potentials (dipolar excitation, quadrupolar excitation, and quadrupolar trapping) are closely approached by the potentials generated by the ''matrix-shimmed'' trap (Fig. 12). For example, $\beta_{\text{dipolar}} \approx 1$ for the ''matrix-shimmed'' trap. The ''matrix-shimmed'' trap consists of a cubic trap in which each side is segmented into a 5×5 grid for a total of 150 electrodes. A near-perfect potential is created by applying the appropriate voltage to each of these electrodes. The ''matrix-shimmed'' trap is an example of inverse logic and is discussed in the ion trap review article by Guan (Guan and Marshall, 1995). Although the matrix-shimmed trap is near-perfect in trapping, dipolar excitation, and quadrupolar excitation potential *shape*, its actual construction necessarily adds so much capacitance that its excitation and detection efficiency are unacceptably low.

VIII. MASS RESOLVING POWER, MASS RESOLUTION, AND MASS ACCURACY

From the first derivative of Eq. (4) with respect to m,

$$\frac{d\omega_c}{dm} = \frac{-qB_0}{m^2} = -\frac{\omega_c}{m} \tag{37}$$

we obtain the useful relation,

$$\frac{\omega_c}{d\omega_c} = -\frac{m}{dm}. \tag{38a}$$

It is usual in all types of Fourier transform spectroscopy to define *resolution* as the full width of a spectral peak at half-maximum peak height: namely, $\Delta\omega_{50\%}$ or $\Delta m_{50\%}$ for frequency-domain or mass-domain FT-ICR spectra, because a valley just begins to appear between two peaks of equal height and shape when they are separated by slightly more than $\Delta\omega_{50\%}$ or $\Delta m_{50\%}$. *Resolving power* is defined as $\omega/\Delta\omega_{50\%}$ or $m/\Delta m_{50\%}$, respectively. Equation (38) shows that frequency resolving power and mass resolving power in ICR mass spectroscopy are the same (except for a minus sign).

Because the frequency of an FT-ICR mass spectral peak is approximately qB_0/m, experimental mass resolution in Eq. (38) can be expressed as

$$\boxed{\frac{m}{\Delta m_{50\%}} = -\frac{qB_0}{m\Delta\omega_{50\%}}} \quad \text{(S.I. units).} \tag{38b}$$

It is useful to evaluate ICR mass resolution for either $T \gg \tau$ (high-pressure limit) or $T \ll \tau$, where T is the time-domain acquisition period and τ is the time-domain exponential damping constant [Eq. (19)]. The results are shown in Table 2. At the low-pressure limit, the time-domain ICR signal persists, undamped, throughout the acquisition period, T. At the high-pressure limit, the ICR time-domain signal damps essentially to zero during the acquisition period.

In the low-pressure limit, the corresponding FT-ICR mass spectral peak width is independent of m/z. Thus, as m/z increases, the peak *width* remains relatively constant, but the peaks are *closer together*, because ICR frequency varies inversely with m/z. That is why [see Eq. (38) and Table 2], for a given ion-neutral collision frequency, ICR mass resolving power (at constant B_0, for a given $T_{\text{acq'n}}$) varies *inversely* with m/z, as shown in Fig. 15.

It is worth noting that Fig. 15 applies to other magnet-based mass separators (notably ''magnetic sector'' mass spectrometers). However, in magnetic sector mass spectrometry, it is usual to vary the magnetic field strength in order to bring ions of a given m/z into focus. In that case, magnetic sector mass resolving power might follow one of the dashed lines in Fig. 15 (i.e., if FT-ICR and magnetic sector mass resolving power are the same at m/z 1000, then the sector resolving power will remain constant throughout the m/z range, whereas the FT-ICR resolving power will increase with decreasing m/z). Thus, FT-ICR MS achieves the highest mass resolution possible for magnet-based mass analysis by operating at the maximum magnetic field strength throughout the mass range. (A fixed-field magnet also produces a spatially more homogeneous field, thereby further increasing mass resolving power.)

IX. UPPER MASS AND ENERGY LIMIT(S)

A. Trap Dimension Mass Limit

Because an ion trap must contain ''side'' electrodes in order to provide for excitation and/or detection of the ICR signal, it is clear that the ultimate upper mass limit is the mass at which the ion cyclotron radius of a thermal ion reaches the radius of the trap. Equation (7) gives the cyclotron radius of an ion of average thermal translational en-

TABLE 2. FT-ICR mass resolution, $\Delta m_{50\%}$, and mass resolving power, $m/\Delta m_{50\%}$, in which $\Delta m_{50\%}$ is the full magnitude-mode FT-ICR mass spectral peak width at half-maximum peak height (Marshall et al., 1979). $T_{\text{acq'n}}$ is time-domain ICR signal acquisition period, and τ is the collisional damping constant [Eq. (19)].

	Low-pressure ($T_{\text{acq'n}} \ll \tau$)	High-pressure ($T_{\text{acq'n}} \gg \tau$)	
$\Delta m_{50\%}$	$\dfrac{7.583\ m^2}{q\ B_0\ T_{\text{acq'n}}}$	$\dfrac{2\sqrt{3}\ m^2}{q\ B_0\ \tau}$	(S.I. units)
$\Delta m_{50\%}$	$\dfrac{7.859 \times 10^{-8}\ m^2}{z\ B_0\ T_{\text{acq'n}}}$	$\dfrac{3.590 \times 10^{-8}\ m^2}{z\ B_0\ \tau}$	(m/z in u per elementary charge)
$\dfrac{m}{\Delta m_{50\%}}$	$\dfrac{0.132\ q\ B_0\ T_{\text{acq'n}}}{m}$	$\dfrac{q\ B_0\ \tau}{2\sqrt{3}\ m}$	(S.I. units)
$\dfrac{m}{\Delta m_{50\%}}$	$\dfrac{1.274 \times 10^7\ z\ B_0\ T_{\text{acq'n}}}{m}$	$\dfrac{2.785 \times 10^7\ z\ B_0\ \tau}{m}$	(m/z in u per elementary charge)

ergy, kT, from which we can solve for the highest mass ion for which the cyclotron radius is less than the trap radius, $d/2$. Rewriting Eq. (7),

$$m_{\text{upper}} = \frac{q^2 B_0^2 r_{\text{max}}^2}{2kT} \quad \text{(S.I. units)} \tag{39a}$$

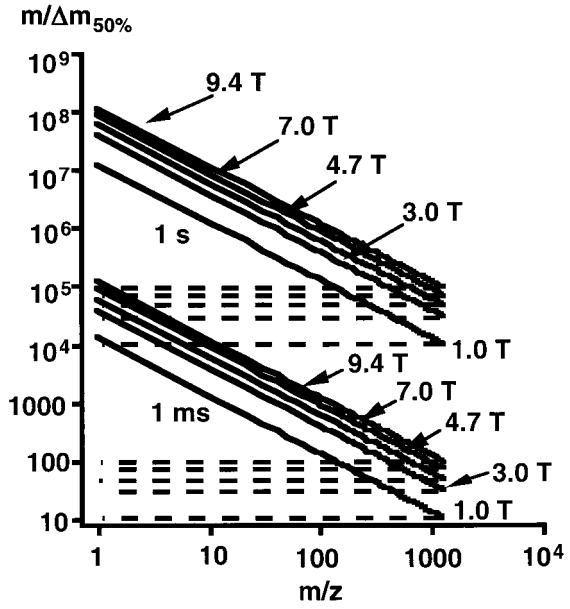

FIGURE 15. FT/ICR theoretical mass resolving power at 1.0, 3.0, 4.7, 7.0, and 9.4 tesla as a function of mass-to-charge ratio, m/z, in u per elementary charge, in the low-pressure limit (i.e., no ion-neutral collisions during the detection period), for $T_{\text{acq'n}} = 1$ ms or 1 s, and a fixed ion-neutral collision frequency. Although mass resolving power decreases with increasing m/z, mass resolution can be spectacularly high if the time-domain acquisition period is long enough. The dashed lines indicate mass resolving power for magnetic field-swept instruments (e.g., magnetic sectors).

$$\boxed{m_{\text{upper}} = \frac{5.598 \times 10^{11} z^2 B_0 r_{\text{max}}^2}{T}}$$

$$\left(\begin{matrix} r \text{ in m; } B_0 \text{ in tesla; } m \text{ in u; } T \text{ in K;} \\ z \text{ in multiples of elementary charge} \end{matrix}\right), \tag{39b}$$

we find that at 7.0 tesla, the upper mass limit for a singly charged room-temperature ion would be ~5.89 megaDalton in a trap of one-inch cross-sectional radius. Of course, the actual upper mass limit will be smaller, because ions must begin with an ICR orbital radius much smaller than that of the trap to generate a detectable coherent signal by exciting the ion's cyclotron orbital motion to a larger radius for detection.

B. Trapping Potential Mass Limit

Equation (39) is valid only in the absence of an electric field (from either the applied electrostatic trapping potential or Coulomb repulsions between ions). In the presence of a three-dimensional axial quadrupolar electrostatic trapping potential, Fig. 14 shows the magnetron, reduced cyclotron, and trapping oscillation frequencies as a function of m/z. Analysis of Eqs. (31) shows that the magnetron and reduced cyclotron frequencies converge to a common value, $\omega_+ = \omega_- = \omega_c/2 = qB_0/2m$, at the so-called ''critical'' m/z (Ledford et al., 1984), namely, when

$$\left(\frac{\omega_c}{2}\right)^2 = \frac{\omega_z^2}{2} \tag{40}$$

or

$$m_{\text{critical}} = \frac{qB_0^2 a^2}{4V_{\text{trap}}\alpha} \quad \text{(S.I. units)} \tag{41a}$$

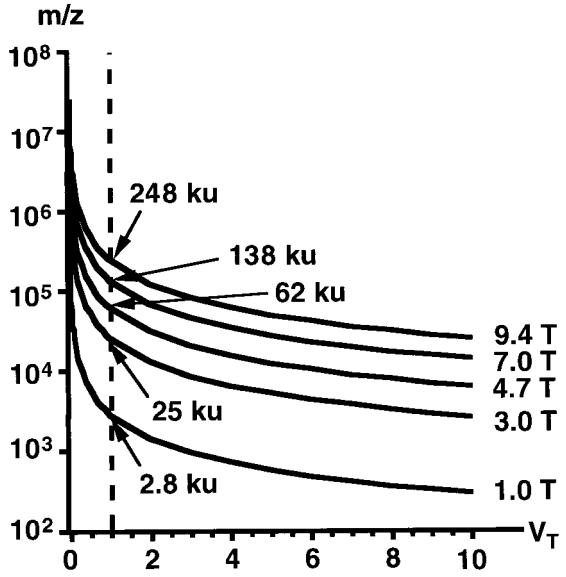

FIGURE 16. Upper mass limit for a singly charged ion in a cubic Penning trap, for each of five common magnetic field strengths: 1.0, 3.0, 4.7, 7.0, and 9.4*T*. At $V_T = 1V$, each arrow denotes the highest *m*/*z* for which an ion has a stable orbit, independent of ion initial velocity (temperature).

$$\boxed{m_{\text{critical}} = \frac{1.20607 \times 10^7 z B_0^2 a^2}{V_{\text{trap}} \alpha}}$$

$$\left(\begin{array}{l} a \text{ in m; } B_0 \text{ in T; } m \text{ in u; } V_{\text{trap}} \text{ in volts;} \\ z \text{ in multiples of elementary charge} \end{array}\right). \quad (41b)$$

For $m/z > m_{\text{critical}}$, ion cyclotron motion is no longer stable, and the ion spirals outward until it is lost from the trap. For example, at 7.0 tesla, for $V_{\text{trap}} = 1$ volt applied to a cubic trap ($\alpha = 2.77373$) of $a = 2.54$ cm, $m_{\text{critical}} = 274{,}000$ *z*. Figure 16 shows the dependence of m_{critical} on trapping voltage, at each of five magnetic field strengths. (The actual upper mass limit in each case is slightly lower, if we specify that (say) 99% of thermal ions fit within the one-inch separation between the detector electrodes.) Figure 16 also shows the desirability of cooling the ions so that the trapping potential may be lowered, thereby increasing the upper mass limit.

C. Trapping Potential Energy Limit; Space Charge and the Peak Coalescence Mass Limit

Obviously, ions with translational energy higher than the potential well depth (which in turn scales linearly with the trapping potential applied to each end cap electrode) can escape axially from the trap. That problem may be solved by increasing the trapping voltage; however, it is also possible to trap too many ions. In fact, when more than ~10,000 ions are present in the trap, it becomes necessary to consider the static and dynamic effects of ion–ion repulsions. It can be shown that, in a spatially uniform static electromagnetic field, Coulomb repulsions between ions do not affect the ICR orbital frequency of the ion packet (Wineland & Dehmelt, 1975). However, in the spatially *nonuniform* electromagnetic field of a typical ion trap, Coulomb repulsions can shift and broaden FT-ICR mass spectral peaks by pushing like-charge ions apart into regions of a different applied external electric or magnetic field.

Peak coalescence (i.e., observation of a single FT-ICR mass spectral peak whose width is narrower than the separation between the cyclotron frequencies of ions of two different *m*/*z*) occurs when two ion clouds have sufficiently large ion populations and very similar mass-to-charge ratios (see Fig. 17). Theoretically, for two very long cylindrical ion clouds whose single-ion cyclotron (R_c) and ion cloud radii (ρ_c) are initially overlapping, the ion clouds coalesce if the difference in cyclotron frequency, $\omega_2 - \omega_1$, between the two clouds is

$$\Delta\omega_c < \frac{N_1 q_1 + N_2 q_2}{2\pi^2 \varepsilon_0 L B_0 R_c s_{\text{eff}}}, \quad (42)$$

in which ε_0 is the vacuum permittivity, $N_1 q_1$ or $N_2 q_2$ is the total charge contained in each cylinder, L is the length of cylinder, and B_0 is the magnetic field induction. $s_{\text{eff}} \approx 1.04$ ρ_c is calculated numerically, based on an initial separation between the two ion clouds of the order of the ion cloud radius ρ_c (Mitchell and Smith, 1995). Thus, the tendency for two ion clouds to coalesce to a single experimentally observable ion cyclotron frequency varies directly with the number of ions in each cloud, and inversely with magnetic field strength and ion cyclotron orbital radius.

Furthermore, one can determine the maximum molecular weight at which coalescence first occurs from (Mitchell and Smith, 1996):

$$m_{\text{max}} \approx 3.2\, B_0 \sqrt{\frac{\varepsilon_0 L R_c \rho_c \Delta m}{N_{\text{ave}}}} \quad \text{(S.I. units)} \quad (43a)$$

$$m_{\text{max}} \approx 2.33327 \times 10^5 B_0 \sqrt{\frac{L R_c \rho_c \Delta m}{N_{\text{ave}}}} \quad (L, R_c, \rho_c \text{ in cm, } m \text{ in u}) \quad (43b)$$

in which N_{ave} is $N_1 + N_2/2$ is the average number of ions in the two clouds. Equation (43) leads to a particularly useful theoretical prediction, namely, that *the highest mass at which ions whose masses differ by one Da begin to coalesce is* ~10,000 B_0 Da (Mitchell and Smith, 1996). Although based on a highly idealized theoretical model

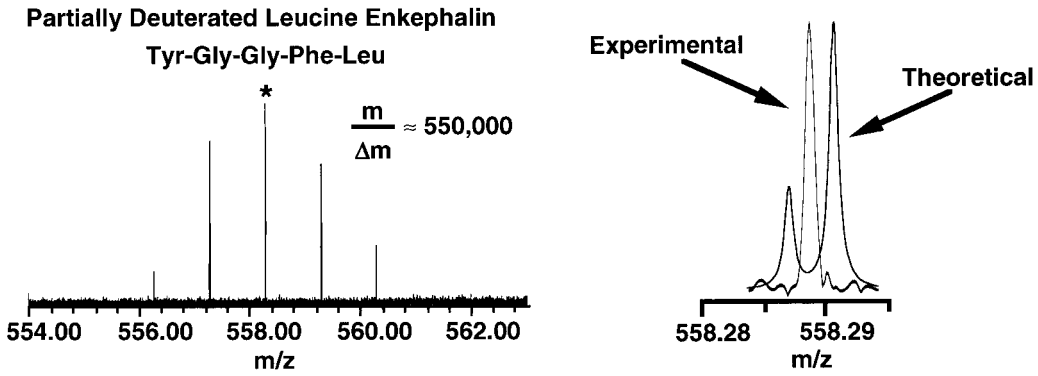

FIGURE 17. Coulomb-mediated peak coalescence. Left: MALDI FT-ICR magnitude-mode mass spectrum of quasimolecular ions, $(M + H)^+$, of deuterated leucine enkephalin. Although mass resolving power greater than 550,000 has been achieved (see Experimental peak in right spectrum), the $^{12}C^2H/^{13}C^1H$ doublet is not resolved (see Theoretical doublet computed from two magnitude-mode Lorentzians at a resolving power of $m/\Delta m_{50\%} \approx 550{,}000$ in right panel), due to the Coulomb interaction of ions of two nearly identical mass-to-charge ratios. (Reproduced, with permission, from Pasa-Tolic et al. (Pasa-Tolic et al., 1995)).

(and, therefore, not to be taken too literally), Mitchell's result provides good insight into the variables that affect peak coalescence.

X. ION SOURCES

A. Internal Ionization

Successful application of the FT-ICR MS technique requires ionization and trapping of the species of interest. For volatile compounds, these processes may be achieved by leaking the corresponding neutral vapor into the volume of the ion trap (either through a valve or by applying less volatile substances to a probe surface, positioning the probe adjacent to the ion trap, and heating to vaporize the substance) and ionizing *in situ* (known as internal ionization). The most common internal ionization technique is electron ionization (photoionization is also in use). In electron ionization (EI), an electron beam of controllable energy and current (typically 70 eV and $\sim$1 μA) is directed through the center of the ion trap for a specified time period. The interaction between the electrons and neutral molecules can result in either the ejection of a valence electron to form positive ions or (for very low energy electrons) electron capture to form negative ions. The electron beam can also be used to perform chemical ionization (CI), in which a suitable reagent is ionized by the electron beam and undergoes proton or electron transfer to form a chemically ionized analyte. Photoionization (PI) is typically performed in the same manner but with a suitable light source (i.e., laser, arc lamp, etc.) directed along the central axis of the ion trap (although not required, ions are almost always formed or injected along the central trap axis for optimal FT-ICR performance). These techniques were the first to be implemented with FT-ICR mass analysis, and have provided ions for a voluminous number of studies that relate to ion–molecule reaction pathways, ion structure and energetics, kinetics, and compound identification (Asamoto and Dunbar, 1991; Chiarelli and Gross, 1988; Eller and Schwarz, 1991; Freiser, 1988; Freiser, 1996; Nibbering, 1990).

B. External Ionization

Although internal ionization methods encompass a wide range of experiments, it is often desirable to couple FT-ICR mass analysis with ion sources that form ions outside the trap, mainly because nonvolatile substances that are not amenable to heating can be effectively desorbed into the gas phase and ionized (i.e., metals, peptides, proteins, oligonucleotides, oligosaccharides, lipids, synthetic polymers, etc.). These external (to the ICR trap) ionization methods may be divided into two categories. In the first, the nonvolatile substance is deposited on a probe surface and the probe is positioned adjacent to the ion trap. A desorption/ionization event follows and the resulting ions can be directed toward the trap and captured. Examples include laser desorption/ionization [or laser desorption of neutrals followed by electron ionization (Lubman, 1990)] and matrix-assisted laser desorption/ionization (MALDI) (Castoro et al., 1992; Hettich and Buchanan, 1991), as well as many others (Amster et al., 1987; Castro and Russell, 1984; Hill et al., 1991; Wang et al., 1990; Williams and McLafferty, 1990). The second class of external ionization techniques operates at such a high pressure ($>$1 torr) that the ion source must be separated from the ion trap by several stages of differential pumping in order to

achieve the necessarily low pressure ($<1 \times 10^{-8}$ torr) required for optimal mass analysis. These methods include electrospray ionization (Henry and McLafferty, 1990; Henry et al., 1989), cluster sources (Alford et al., 1986), and high-pressure sources (Hop et al., 1990; Kofel and McMahon, 1990). The multiple pumping stages usually require that the source be located outside the solenoidal ICR magnet [see (Hofstadler and Laude, 1992) for an exception] so that the ions formed by these methods are injected through the magnetic fringe field by a suitable ion guide [electrostatic Einzel lenses (Kofel et al., 1986), multipole rf ion guides (McIver et al., 1985), and dc wire ion guides (Limbach et al., 1993) have been used]. Although more complex, the ion guides have worked well enough so that many ionization techniques that can be located inside the magnet have also been implemented outside the magnet (Marto et al., 1994; McIver et al., 1994), usually for convenience in accessing the ion source.

C. Chromatographic Interfaces

FT-ICR MS is capable of powerful mixture analysis due to its high mass range and ultrahigh mass resolving power. However, in many cases it is still desirable to couple a chromatographic interface to the mass spectrometer for sample purification, preconcentration, and mixture separation. The first separation technique to be coupled with FT-ICR was gas chromatography (GC) (Larsen et al., 1986). The GC effluent is admitted into the ion trap region of the vacuum chamber, and ions are formed with an electron beam. More recent efforts have focused on liquid chromatography (LC) (Senko et al., 1997; Stacey et al., 1994; Stockton et al., 1991) and capillary electrophoresis (CE) (Hofstadler et al., 1993); both were coupled to the mass spectrometer by use of electrospray ionization. These couplings have produced exciting new advances in the analysis of biopolymers that are present in complex biological matrices (Hofstadler et al., 1996; Senko et al., 1997).

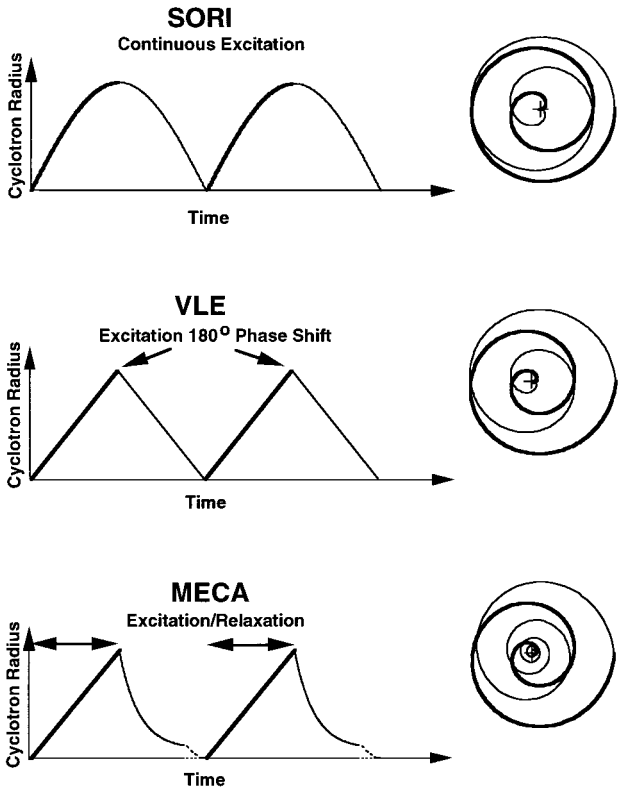

FIGURE 18. Time evolution of ion cyclotron radius (left) and ion *xy*-trajectory (right) for each of three ICR techniques for ion multiple activation based on repeated single-frequency dipolar excitation for collision-induced dissociation (CID). In sustained off-resonance irradiation (SORI) (Gauthier et al., 1991), ions of a selected *m*/*z* ratio are alternately excited and de-excited due to the difference between the excitation frequency and the ion cyclotron frequency. In very low energy (VLE) CID (Boering et al., 1992), ions are alternately excited and de-excited by resonant excitation whose phase alternates bimodally between 0° and 180°. In multiple excitation for collisional activation (MECA) (Lee et al., 1993), ions are resonantly excited and then allowed to relax by collisions. (Reproduced, with permission, from (Guan and Marshall, 1996).)

XI. MS/MS AND MS^n: CAD (SORI, MECA, VLE), IRMPD, SID, BIRD

Tandem mass spectrometry (MS/MS or MS^n) consists of the activation of primary (''precursor'') ions, dissociation or reaction, followed by mass analysis of the resulting secondary (''product'') ions. In an FT-ICR instrument, activation is commonly achieved by collisions of ions with neutrals [collision-activated dissociation (CAD) or collision-induced dissociation (CID)] (Cody et al., 1982) or surfaces [surface-induced dissociation (SID)] (Castoro et al., 1992; Ijames and Wilkins, 1990; Williams et al., 1990), ultraviolet photodissociation (UVPD) (Bowers et al., 1984), multiphoton infrared photodissociation (IRMPD) (Little et al., 1994; Peiris et al., 1993; Woodlin et al., 1978), or blackbody infrared dissociation (BIRD) (Dunbar and McMahon, 1998). For CAD (CID) of macromolecular ions, the most popular method is sustained off-resonance irradiation (SORI) (Gauthier et al., 1991), although very low-energy (VLE) (Boering et al., 1992) and multiple excitation collisional activation (MECA) (Lee et al., 1993) are also available. Figure 18 shows that SORI, VLE, and MECA each provide for periodic excitation of ion cyclotron radius (and thus ion translational energy) to an adjustable maximum value; SORI tends to be preferred, probably because it is the simplest to implement and tune.

Photodissociation of large biomolecules has also proved effective for biomolecule characterization. Typically, IR (10.6 μm) laser photons are used for ''slow heating,'' and fragments similar to those obtained by CAD are

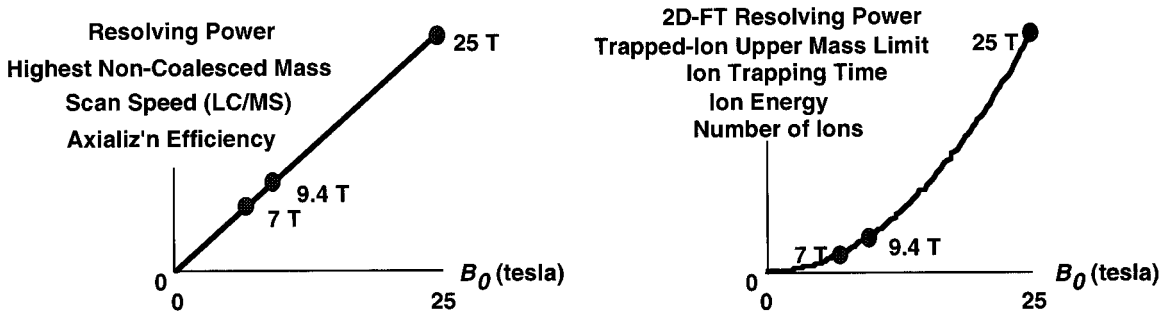

FIGURE 19. FT-ICR mass spectrometry performance parameters as a function of applied static magnetic field induction, B_0. Left: Parameters that increase linearly with increasing magnetic field. Right: Parameters that increase quadratically with increasing magnetic field.

produced (Little et al., 1994). One advantage of IRMPD is that gas pulses are not necessary, so that high-resolution FT-ICR detection can occur quickly after dissociation (no pumpdown is required). An alternative to laser photodissociation takes advantage of the blackbody radiation produced by a heated vacuum chamber (BIRD) (Price et al., 1996). Ions are confined in the hot ICR trap (10–1000 s), where ion structure- and temperature-dependent interaction with the blackbody radiation occurs. A unique feature of BIRD is that the ion cloud assumes a known (i.e., Boltzmann) and controllable internal energy distribution. Thus, information on dissociation energetics and mechanisms can be obtained from the temperature-dependence of the unimolecular dissociation rate constants (Price et al., 1996).

Finally, SID has been investigated as a probe of ion structure by FT-ICR MS. The advantage of SID is the potential for high internal energy deposition with a relatively narrow distribution. However, results to date indicate that the collection of product ions is difficult, and that unique structural information is rarely obtained (Castoro et al., 1992; Chorush et al., 1995; Ijames and Wilkins, 1990; Williams et al., 1990).

XII. ADVANTAGES OF A HIGH MAGNETIC FIELD

We noted above that mass resolving power in Fourier transform ion cyclotron resonance mass spectrometry (FT-ICR MS) increases linearly with increasing applied magnetic field induction, B, for fixed ion-neutral collision frequency. In fact, *eight* other FT-ICR primary performance parameters theoretically also increase linearly (quadrupolar axialization efficiency, data acquisition speed, upper mass limit for peak coalescence) or quadratically (upper mass limit due to trapping potential, maximum ion kinetic energy, maximum number of trapped ions, maximum ion trapping duration, two-dimensional FT-ICR mass resolving power) with increasing B (see Fig. 19). [Two-dimensional FT-ICR MS, like two-dimensional ''NOESY'' nuclear magnetic resonance spectroscopy, provides an automated method for determining ion–molecule reaction pathways, kinetics, and equilibria simultaneously for all primary (''precursor'') ions in a mixture (Haebel et al., 1995; Pfändler et al., 1988; Ross et al., 1993)]. The origin of (and conditions for) the magnetic field dependence of each of these parameters have been collected and discussed (Marshall and Guan, 1996; Mitchell and Smith, 1996). These fundamental advantages lead to a corollary improvement in other FT-ICR performance parameters: e.g., signal-to-noise ratio, dynamic range, mass accuracy, ion remeasurement efficiency, and mass selectivity for MS/MS. Finally, these various advantages may be exploited in combination, so as to produce an even higher enhancement in a particular parameter: e.g., signal-to-noise ratio can improve by more than a factor of B^2 if mass resolving power is fixed at the same value as at lower magnetic field (Senko et al., 1996).

XIII. FOURIER TRANSFORM SPECTROSCOPY ASPECTS

FT-ICR mass spectrometry shares many common conceptual and data reduction features with other types of FT spectroscopy, as discussed in depth in a recent monograph (Marshall and Verdun, 1990). The homology between FT-ICR and FT-NMR is deep and virtually complete (Marshall, 1996). The most unique advantage of FT-ICR as a mass analyzer is that the ion mass-to-charge ratio is experimentally manifested as a *frequency*. Because frequency can be measured more accurately than any other experimental parameter, ICR MS, therefore, offers an inherently higher resolution (and thus higher mass accuracy) than any other type of mass measurement. The introduction of FT techniques to ICR MS (Comisarow and Marshall, 1974; Comisarow and Marshall, 1974) brought not only the Fellgett (multichannel, open-

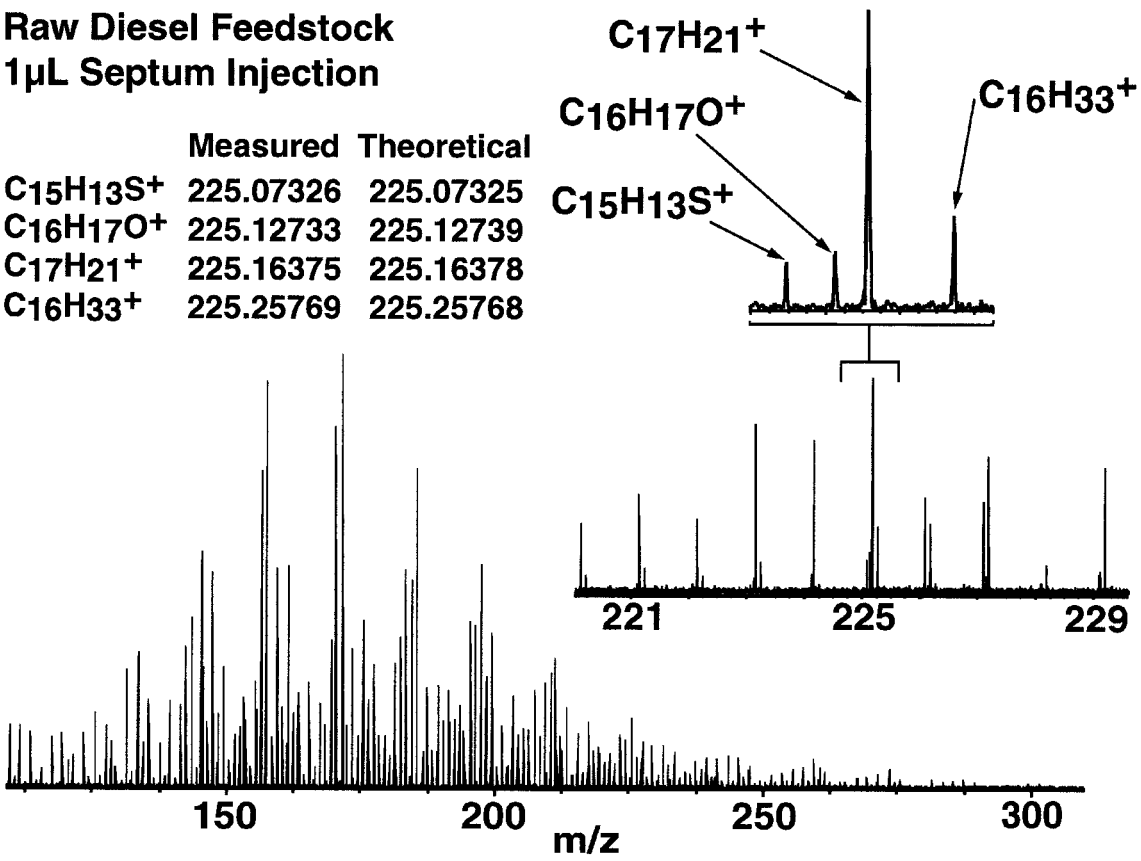

FIGURE 20. Low-energy electron impact ionization 5.6 T FT-ICR mass spectrum, showing ~500 resolved peaks, for a 1 μL septum injection of raw diesel feedstock. The inset mass window shows resolution of four ions of different elemental composition at the same nominal mass, each identified with mass accuracy < 0.3 ppm at a mass resolving power $m/\Delta m_{50\%} \approx 100{,}000$. Data kindly provided by R. Rodgers.

ing the exit slit) advantages of increased speed (factor of 10,000) or increased sensitivity (factor of 100), but also the advantages of fixed magnetic field rather than swept field (Comisarow, 1978); namely, increased mass resolution (factor of 10,000) and increased mass range (factor of 500). Applications that derive from these advantages include determination of chemical formulas, particularly in complex mixtures; detection limit in the attomole range; and multistage MS^n.

FT manifestations in ICR include: Nyquist sampling and foldover (Wang and Marshall, 1988), fast Fourier transformation, zero-filling (Comisarow and Melka, 1979), ''windowing'' or apodization (Marshall and Verdun, 1990), deconvolution (Marshall, 1979; Marshall and Roe, 1980; Zhang et al., 1997), oversampling (Alber and Marshall, 1990), two-dimensional Hadamard (Williams et al., 1990) or Fourier (Ross et al., 1993) MS/MS, etc. In addition, various non-FT methods for obtaining a frequency-domain (and thus mass-domain) spectrum from a time-domain ''interferogram'' ICR signal include: the Hartley transform (a way of performing a Fourier transform on real-only data) (Williams and Marshall, 1989; Williams and Marshall, 1992), the Bayesian maximum entropy method (MEM) (Meier and Marshall, 1990; Meier and Marshall, 1991), and linear prediction (Guan and Marshall, 1997; Loo et al., 1990).

However, several aspects of FT-ICR data reduction differ from those of FT-interferometry or FT-NMR spectroscopy. Notably, the phasing of FT-ICR spectra over a broad frequency range is difficult (Craig et al., 1987); thus, spectra are usually reported in magnitude-mode rather than absorption-mode (Comisarow and Marshall, 1974). As a result, resolving power is lower than for absorption-mode by a factor ranging from $\sim \sqrt{3}$ (Lorentzian peak shape) to 2 (sinc peak shape) (Marshall et al., 1979), and new peak-fitting algorithms have been developed (Serreqi and Comisarow, 1987). Apodization of magnitude-mode spectra has been performed by means of magnitude-mode multiple-derivative techniques (Kim and Marshall, 1995). Moreover, FT-NMR is conducted exclusively in heterodyne-mode, whereas FT-ICR MS is often performed by sampling the ICR signal directly without heterodyning. Due

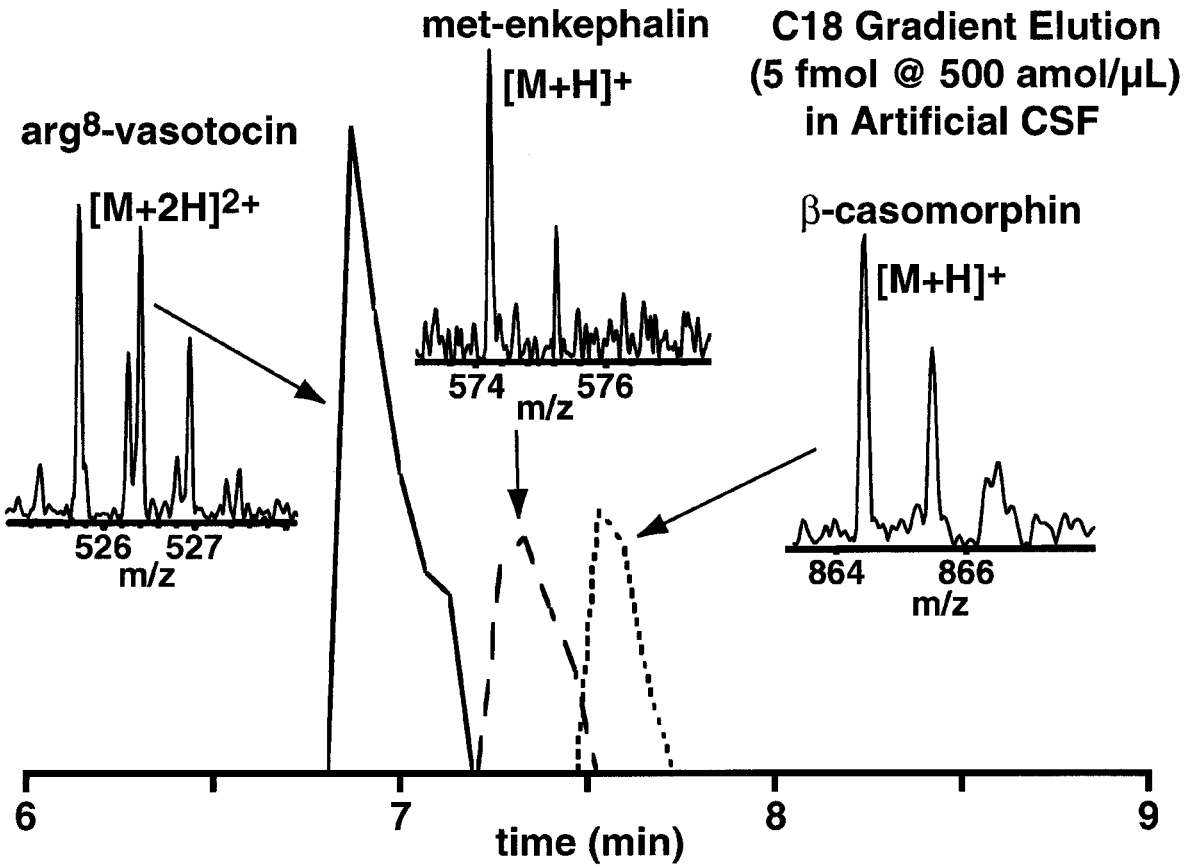

FIGURE 21. True gradient elution of 5 fmol each of an equimolar mixture of three peptides: Arg^8-vasotocin, methionine enkephalin, and β-casomorphin. Samples were dissolved in artificial cerebrospinal fluid at 500 attomol/μL each and loaded (10 μL) onto a C18 packed micro-ESI needle. The reconstructed ion chromatogram is shown below, with ESI FT-ICR mass spectra of individual peptide spectra shown as insets. Reproduced from (Emmett et al., 1998).

to the need for massively large data sets (several megawords of time-domain data) to take advantage of potentially ultrahigh mass resolving power over a wide mass range, data clipping (to as low as 1 bit/word) has been demonstrated with only modest distortion of the FT spectrum (Hsu et al., 1985). Finally, the ICR time-domain signal typically exhibits nonexponential damping (Guan et al., 1998); hence, it is common to apodize the time-domain signal with a window function (e.g., Blackman–Harris) that preferentially damps the initial portion of the time-domain signal prior to Fourier transformation.

XIV. RELATION TO PAUL (QUADRUPOLE) ION TRAP

The close relation between Penning (ICR) and Paul (quadrupole) ion traps is perhaps most evident from the 1989 Nobel Prize, which was shared by Dehmelt and Paul, the two most famous developers of the two techniques. Many trapped-ion techniques first introduced in FT-ICR have since been adapted to the Paul trap: e.g., collision-induced dissociation of trapped ions (Louris et al., 1990), mass-selective ion ejection (Goeringer et al., 1992), frequency-sweep excitation (McLuckey et al., 1991), stored-waveform excitation/ejection (Guan and Marshall, 1993; Guan and Marshall, 1996; Julian and Cooks, 1993; Soni and Cooks, 1994), Fourier transform detection of an induced image current (Soni et al., 1996; Syka and Fies, 1988), and the interfacing of various ion sources to the mass analyzer.

XV. SELECTED APPLICATIONS

A. Elemental Composition from Accurate Mass Measurement

A powerful advantage of FT-ICR over other mass analyzers is its accurate mass capability. For singly charged

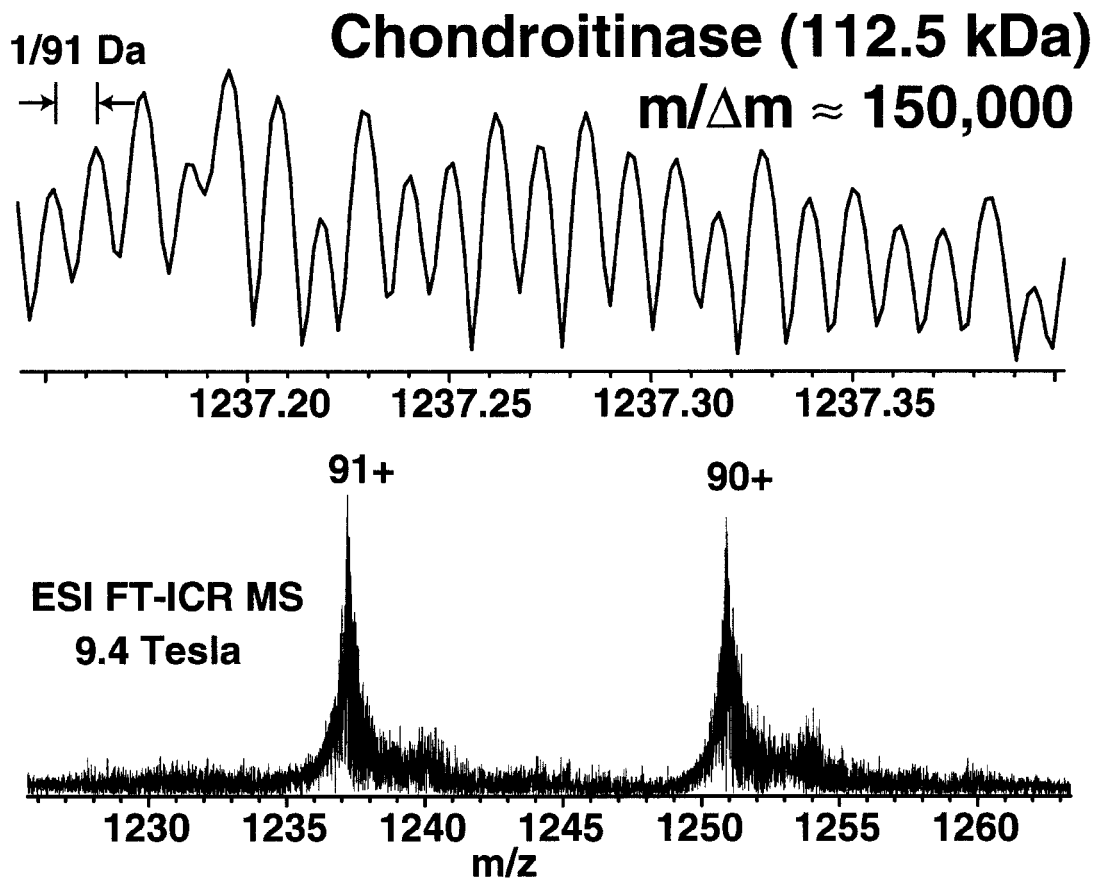

FIGURE 22. ESI FT-ICR mass spectra of chondroitinase I. Bottom: Heterodyne data for SWIFT-isolated ions, $1226 < m/z < 1273$, with external ion accumulation (Senko et al., 1997), from 10 co-added time-domain signals; the peaks at m/z 1240 and 1254 correspond to an unidentified adduct of ~260 Da. Top: Mass scale-expansion showing unit mass resolution of the isotopic distribution of the $z = 91$ charge state. Data kindly provided by N. Kelleher and described in detail elsewhere (Kelleher et al., 1997).

ions of <700 Da, a unique elemental composition can be assigned directly from the measured mass if ~1 ppm mass accuracy can be achieved (Guan et al., 1996; Zubarev et al., 1996). An example is shown in Fig. 20, in which electron ionization FT-ICR mass analysis of raw diesel fuel feedstock resolves ~500 singly charged ion masses in the range, 90–300 Da. The ultrahigh resolving power afforded by FT-ICR MS reveals several different species at each nominal mass. With proper mass calibration [see Eq. (32)], the elemental composition of each species can be assigned unambiguously based on sub-ppm mass accuracy. Elemental composition is critical in such analyses, because it is important to identify and monitor sulfur- and nitrogen-containing species as they are removed during the fuel purification process.

B. Detection Limit for Biological Analysis

A fundamental limit of FT-ICR broadband image current detection is that typically ~100 ions of a given mass-to-charge ratio are required to induce a measurable signal. ''Ion counting'' (destructive-detection) mass spectrometers are, therefore, inherently more sensitive. However, the FT-ICR detection limit can still be spectacularly low. With capillary electrophoresis (CE) coupling, Hofstadler et al. acquired hemoglobin mass spectra from a single red blood cell that contains ~450 amol of hemoglobin (Hofstadler et al., 1996). An even *lower* detection limit has been achieved in McLafferty's laboratory, where CE FT-ICR mass spectra have been observed from sub-attomole protein samples (Valaskovic et al., 1996). Further, the same researchers used a CAD spectrum from 9 amol of carbonic anhydrase and database searching to unambiguously identify the protein in spite of N-terminal acetylation. Although *lower* detection limits have been obtained with other mass analyzers, the unique combination afforded by accurate mass measurement, ultrahigh resolution, and nondestructive detection that allow for MS^n in combination with a *very low* detection limit makes FT-ICR extremely attractive for biological analysis.

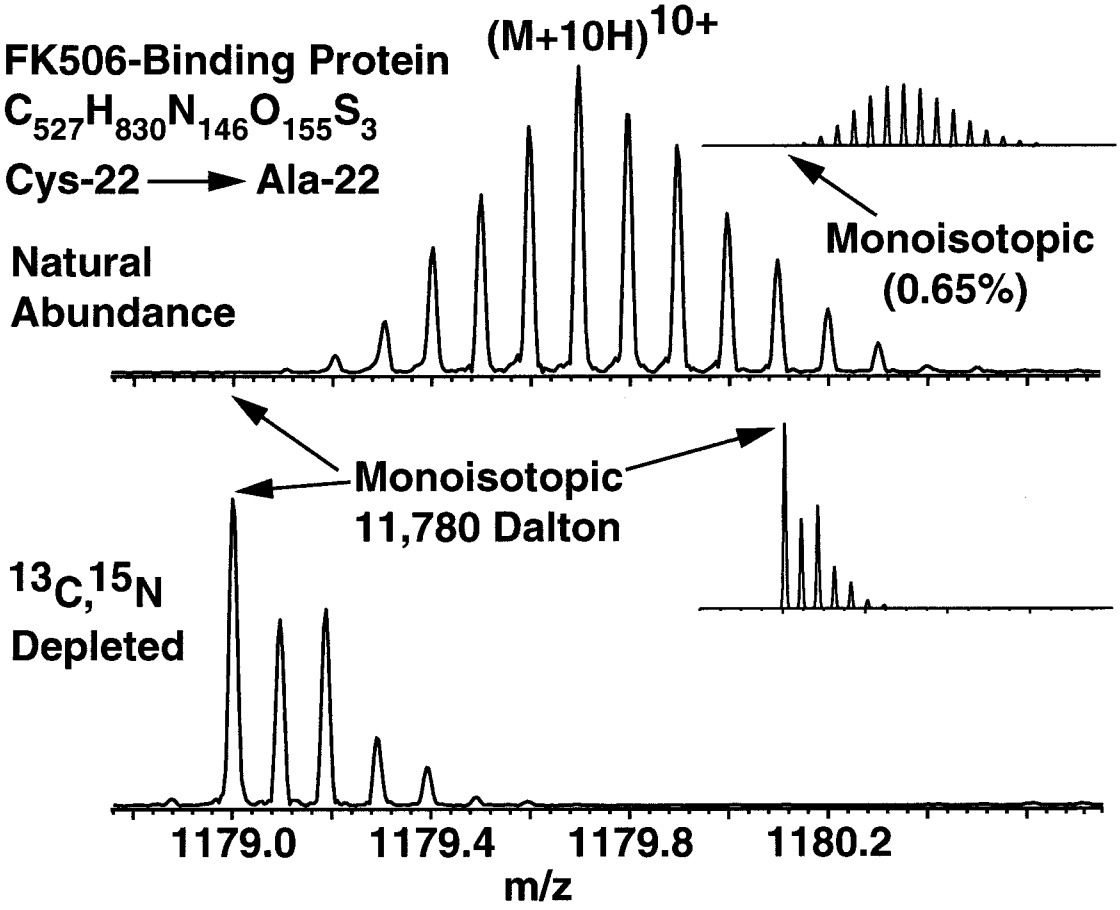

FIGURE 23. Electrospray ionization Fourier transform ion cyclotron resonance mass spectra (9.4 tesla) of a mutant (C22A) FK506-binding protein. Top: Natural-abundance isotopic distribution (~98.89% ^{12}C; ~99.63% ^{14}N). Bottom: Isotopic distribution for the same protein grown on a medium with 99.95% ^{12}C and 99.99% ^{14}N. Insets: Isotopic distributions calculated (same vertical scale) from the chemical formula for natural-abundance (top) and ^{13}C, ^{15}N doubly-depleted (bottom) FK506 binding protein. Reproduced, with permission, from (Marshall et al., 1997).

A key feature common to the impressive results from Smith and McLafferty is the CE coupling. However, a major disadvantage of CE sample introduction is the requirement of a fairly concentrated analyte solution. LC FT-ICR is an attractive alternative for the very dilute solutions that are often encountered in biological samples. Figure 21 shows a selected-ion chromatogram and mass spectra from the LC FT-ICR mass analysis of a three-component peptide mixture (Emmett et al., 1998). Each of those peptides was present at 500 pM concentration in a 100 mM salt aqueous matrix! Sample loading onto a specially designed nano-LC column/microelectrospray tip facilitates sample desalting, preconcentration, and gradient separation (Emmett and Caprioli, 1994).

C. High Mass

The multiple-charging that is inherent to electrospray ionization (ESI) has revolutionized the mass analysis of large molecules (Fenn et al., 1989). Typically, the highest mass species carry the greatest number of charges, thereby yielding ions with mass-to-charge ratio ($500 < m/z < 2500$) especially favorable for FT-ICR detection even at very high ion mass. The combination of electrospray ionization with FT-ICR detection has yielded striking results in the analysis of large ions. Unit mass resolution and accurate mass analysis are now routine for proteins as large as 67 kDa (Senko et al., 1996; Speir et al., 1995; Wood et al., 1995) and have been achieved for two 112 kDa proteins (Kelleher et al., 1997), the highest-mass molecules for which unit mass resolution has been achieved (see Fig. 22). In that work, the masses of two chondroitinase enzymes were determined with 3 Da accuracy; that information helps to obtain FDA approval for use of the enzymes as drugs. Finally, the trapping and detection of a single 100 Megadalton DNA ion with ~30,000 charges has been achieved (Chen et al., 1995).

D. Isotopic Amplification for Unit Mass Accuracy of Biomacromolecules

Several related problems arise from the presence of multiple isotopes in biological macromolecular ions. First, a typical electrospray-ionized protein can take on about 1 proton per kDa, by protonation of available arginine and lysine residues. Because mass analyzers in general (and ICR in particular) separate ions based on mass-to-charge *ratio* (m/z, in which m is ion mass in u and z is charge in multiples of the elementary charge), the first problem is how to determine charge independent from mass. Fortunately, if the isotopic envelope can be resolved to better than 1 u (as in Fig. 22, top), then adjacent peaks differ by $m/z = 1/z$; ergo, the ion charge may be obtained simply as the reciprocal of the spacing between two adjacent peaks in the m/z spectrum (McLafferty, 1994). Because only FT-ICR MS can resolve such multiplets for macromolecular ions of more than a few kDa, FT-ICR MS is the method of choice for mass analysis of such species.

A second (more vexing) problem is that, even if the m/z for each of the resolved isotopic peaks can be determined to a ppm accuracy, the molecular weight can still be in error by a whole Dalton or more, because (except for the lowest-mass ''monoisotopic'' species—namely, the unique elemental composition for which all carbons are ^{12}C, all nitrogens are ^{14}N, all oxygens are ^{16}O, all sulfurs are ^{32}S, etc.), it is necessary to match the observed isotopic abundance distribution to that predicted for (e.g.) a protein of average amino acid composition (Senko et al., 1995). However, if the relative abundances are just a bit in error, or if the unknown protein differs in composition from the average protein in the database, then the estimated molecular weight can be in error by 1 or more Da.

A simple solution to the above problem is to express a protein from a minimal medium that contains ^{13}C-depleted glucose and ^{15}N-depleted ammonium sulfate. An example is shown in Fig. 23. Simulated and experimental electrospray FT-ICR mass spectra both show that double-depletion of ^{13}C and ^{15}N effectively narrows and shifts the isotopic distribution to the left, so that the monoisotopic species is now prominent and easily identified (Marshall et al., 1997). This technique promises to extend the upper mass limit for protein mass spectrometry by about an order of magnitude, and is optimally exploited only by FT-ICR MS (Marshall et al., 1997). By measuring protein mass accurately to within 1 Da, it becomes possible to count the number of disulfide bridges (—S—S— is 2 Da lighter than 2 —SH); identify deamidation (—NH_2 is 1 Da lighter than —OH); identify post-translational modifications and noncovalent adducts; and identify proteome components directly without prior two-dimensional gel separation.

APPENDIX A. FT-ICR REVIEWS

Books

Buchanan, M. V., Ed. *Fourier Transform Mass Spectrometry: Evolution, Innovation, and Applications, ACS Symp. Series;* American Chemical Society: Washington, D.C., **1987,** 205 pp.

Marshall, A. G.; Verdun, F. R. *Fourier Transforms in NMR, Optical, and Mass Spectrometry: A User's Handbook;* Elsevier: Amsterdam, **1990,** 460 pp.

Asamoto, B.; Dunbar, R. C. *Analytical Applications of Fourier Transform Ion Cyclotron Resonance Mass Spectrometry;* VCH: New York, **1991,** 306 pp.

Journal Special Issues

Pardue, H. L. ''Special issue: Fourier transform mass spectrometry: fundamental aspects and analytical applications.'' *Analyt. Chim. Acta* **1985,** *178,* 158 pp.

Comisarow, M. B.; Nibbering, N. M. M., Eds. ''Special Issue: Fourier Transform Ion Cyclotron Resonance Mass Spectrometry.'' *Int. J. Mass Spectrom. Ion Proc.* **1986,** *72,* 222 pp.

Wilkins, C. L. ''Special issue: Fourier transform mass spectrometry.'' *Trends in Analyt. Chem.* **1994,** *13,* 223–251.

Marshall, A. G. ''Special issue: Fourier transform ion cyclotron resonance mass spectrometry.'' *Int. J. Mass Spectrom. Ion Processes* **1996a,** *137/138,* 410 pp.

Review Articles

Early History of FT-ICR MS

Comisarow, M. B. ''Fourier transform ion cyclotron resonance spectroscopy.'' In *Fourier, Hadamard, and Hilbert Transforms in Chemistry;* Marshall, A. G., Ed.; Plenum: NY, **1982,** 125–146.

Marshall, A. G. ''Fourier transform ion cyclotron resonance mass spectrometry.'' *Acc. Chem. Res.* **1985,** *18,* 316–322.

Comisarow, M. B.; Marshall, A. G. ''The early development of Fourier transform ion cyclotron resonance (FT-ICR) spectroscopy.'' *J. Mass Spectrom.* **1996,** *31,* 581–585.

Marshall, A. G. ''Ion cyclotron resonance mass spectrometry: A brief history.'' In *Encyclopedia of Nuclear Magnetic Resonance;* Grant, D. M.; Harris, R. K., Ed.; Wiley: London, **1996,** *1,* 486–489.

Later FT-ICR MS Developments

Wanczek, K.-P. ''ICR spectrometry—A review of new developments in theory, instrumentation, and applications. I. 1983–1986.'' *Int. J. Mass Spectrom. Ion Proc.* **1989,** *95,* 1–38.

Freiser, B. S. ''Methods for determining metal-ligand and metal-metal bond energies using FTMS.'' In *Bonding Energetics in Organometallic Compounds;* Marks, T. J., Ed.; Amer. Chem. Soc.: Washington, D. C., **1990,** *428,* 55–69.

Speir, J. P.; Gorman, G. S.; Amster, I. J. ''Laser desorption, chemical ionization, and laser desorption/chemical ionization applications with FTMS.'' In *Mass Spectrometry in the Biological Sciences: A Tutorial;* Gross, M. L., Ed.; Kluwer Academic Publishers: Dordrecht, The Netherlands, **1992,** 199–212.

Marshall, A. G.; Schweikhard, L. ''Fourier transform ion cyclotron resonance mass spectrometry: technique developments.'' *Int. J. Mass Spectrom. Ion Processes* **1992,** *118/119,* 37–70.

Nibbering, N. M. M. ''Principles and applications of FTICR mass spectrometry.'' *Analyst* **1992,** *117,* 289–293.

Brenna, J. T.; Creasy, W. R.; Zimmerman, J. A. ''Laser Fourier transform mass spectrometry for polymer characterization.'' *Amer. Chem. Soc. Symp. Ser.* **1993,** *236,* 129–154.

Buchanan, M. V.; Hettich, R. L. ''Characterization of large biomolecules by Fourier transform mass spectrometry.'' *Anal. Chem.* **1993,** *65,* 245A–259A.

Guan, S.; Kim, H. S.; Marshall, A. G.; Wahl, M. C.; Wood, T. D.; Xiang, X. ''Shrink-wrapping an ion cloud for higher-performance Fourier transform ion cyclotron resonance mass spectrometry.'' *Chem. Rev.* **1994,** *94,* 2161–2182.

McLafferty, F. W. ''High-resolution tandem FT mass spectrometry above 10 kDa.'' *Acc. Chem. Res.* **1994,** *27,* 379–386.

Guan, S.; Marshall, A. G. ''Ion traps for FT-ICR/MS: Principles and design of geometric and electric configurations.'' *Int. J. Mass Spectrom. Ion Processes* **1995,** *146/147,* 261–296.

Amster, I. J. ''A tutorial on Fourier transform mass spectrometry.'' *J. Mass Spectrom.* **1996,** *31,* 1325–1337.

Marshall, A. G.; Guan, S. ''Advantages of high magnetic field for FT-ICR mass spectrometry.'' *Rapid Commun. Mass Spectrom.* **1996,** *10,* 1819–1823.

Marshall, A. G. ''Ion cyclotron resonance and nuclear magnetic resonance spectroscopies: Magnetic partners for elucidation of molecular structure and reactivity.'' *Acc. Chem. Res.* **1996,** *9,* 307–316.

Guan, S.; Marshall, A. G. ''Stored waveform inverse Fourier transform (SWIFT) ion excitation in trapped-ion mass spectrometry: theory and applications.'' *Int. J. Mass Spectrom. Ion Processes* **1996,** *157/158,* 5–37.

Dienes, T.; Pastor, S. J.; Schürch, S.; Scott, J. R.; Yao, J.; Cui, S.; Wilkins, C. L. ''Fourier transform mass spectrometry—Advancing years (1992-mid 1996).'' *Mass Spectrom. Rev.* **1996,** *15,* 163–211.

Green, M. K.; Lebrilla, C. B. ''Ion-molecule reactions as probes of gas phase structures of peptides and proteins.'' *Mass Spectrom. Rev.* **1997,** *16,* 53–71.

Other Reviews Cited in the Above Articles

Marshall, A. G.; Comisarow, M. B. ''Fourier and Hadamard transform methods in spectroscopy.'' *Anal. Chem.* **1975,** *47,* 491A.

Marshall, A. G.; Comisarow, M. B. ''Fourier transform methods in spectroscopy.'' *J. Chem. Educ.* **1975,** *52,* 638–641.

Marshall, A. G.; Comisarow, M. B. ''Multichannel methods in spectroscopy.'' In *Transform Techniques in Chemistry;* Griffiths, P. R., Ed.; Plenum: New York, **1978,** 39–68.

Wilkins, C. L. ''Fourier transform mass spectrometry.'' *Anal. Chem.* **1978,** *50,* 493A–498A.

Wilkins, C. L.; Gross, M. L. ''FTMS for analysis.'' *Anal. Chem.* **1981,** *53,* 1661A–1668A.

Marshall, A. G. ''Advantages of transform methods in chemistry.'' In *Fourier, Hadamard, and Hilbert Transforms in Chemistry;* Marshall, A. G., Ed.; Plenum: New York, **1982,** 1–43.

Johlman, C. L.; White, R. L.; Wilkins, C. L. ''Applications of FTMS.'' *Mass Spectrom. Rev.* **1983,** *2,* 389–415.

Marshall, A. G. ''Transform techniques in chemistry.'' In *Physical Methods of Modern Chemical Analysis;* Kuwana, T., Ed.; Academic Press: New York, **1983,** *3,* 57–135.

Gross, M. L.; Rempel, D. L. ''Fourier transform mass spectrometry.'' *Science* **1984,** *226,* 261–268.

Wanczek, K.-P. ''ICR spectrometry—A review.'' *Int. J. Mass Spectrom. Ion Proc.* **1984,** *60,* 11–60.

Comisarow, M. B. ''Fundamental aspects and applications of Fourier-transform ion-cyclotron resonance spectrometry.'' *Anal. Chim. Acta* **1985,** *178,* 1–15.

Freiser, B. S. ''Investigation of the reactions of metal ions and their clusters in the gas phase by laser-ionization FTMS.'' *Talanta* **1985,** *32,* 697–708.

Marshall, A. G. ''Fourier transform ion cyclotron resonance mass spectrometry.'' *Acc. Chem. Res.* **1985,** *18,* 316–322.

Marshall, A. G. ''Fourier transform methods in spectroscopy.'' In *IUCCP Symposium;* Marshall, A. G., Ed.; Texas A&M University Press: College Station, TX, **1985,** 111–134.

Marshall, A. G. ''Fourier transform ion cyclotron resonance mass spectrometry. Potential for biomedical applications.'' In *Mass Spectrometry in the Health and Life Sciences;* Burlingame, A. L., Ed.; Elsevier: Amsterdam, **1985,** *24,* 265–286.

Laude, D. A., Jr.; Johlman, C. L.; Brown, R. S.; Weil, D. A.; Wilkins, C. L. ''FTMS: recent instrument developments and applications.'' *Mass Spectrom. Rev.* **1986,** *5,* 107–166.

Marshall, A. G.; Chen, L.; Hsu, A. T.; Mullen, S. L.; Ricca, T. L.; Santos, I.; Shomo, R. E., II; Wang, T.-C. L.; Weisenberger, C. R. ''Fourier transform ion cyclotron mass spectrometry: New theoretical and experimental developments.'' In *Advances in Mass Spectrometry;* Todd, J. F. J., Ed.; Wiley: New York, **1986,** *1985B,* 927–928.

Marshall, A. G. ''Fourier transform mass spectrometry.'' In *Spectroscopy in the Biomedical Sciences;* Gendreau, R. M., Ed.; CRC Press: Boca Raton, FL, **1986,** 87–105.

Nibbering, N. M. M. ''Experiments with ions in a Fourier transform ion cyclotron resonance mass spectrometer.'' *Comments At. Mol. Phys.* **1986,** *18,* 223–234.

Russell, D. H. ''An evaluation of Fourier transform mass spectrometry for high mass applications.'' *Mass Spectrom. Rev.* **1986,** *5,* 167–189.

Hanson, C. S.; Castro, M. E.; Russell, D. H.; Hunt, D. F.; Shabanowitz, J. ''Fourier transform mass spectrometry of large ($m/z > 5000$) biomolecules.'' In *Fourier Transform Mass Spectrometry: Evolution, Innovation, and Applications;* Buchanan, M. V., Ed.; American Chemical Society: Washington, D. C., **1987,** *359,* 100–115.

Asamoto, B. ''FTMS for industrial problem solving.'' *Spectroscopy* **1988,** *3,* 38–46.

Chiarelli, M. P.; Gross, M. L. ''FTMS for chemical analysis: A brief status report.'' In *Analytical Applications of Spectroscopy;* Creaser, C. S.; Davies, A. M. C., Ed.; Royal Society of Chemistry: London, **1988,** 262–273.

Cody, R. B. ''An overview of MS/MS and FTMS.'' *Analysis* **1988,** *16,* 30–36.

Freiser, B. S. ''Fourier transform mass spectrometry.'' In *Tech-*

niques for the Study of Ion Molecule Reactions; Farrar, J. M.; Saunders, W. H., Jr., Ed.; Wiley: New York, **1988,** *20,* 61–118.

Hanson, C. D.; Kerley, E. L.; Russell, D. H. ''Recent developments in experimental FT/ICR.'' In *Treatise in Analytical Chemistry;* 2nd Ed.; Winefordner, J. D., Ed.; Wiley: New York, **1988,** *11,* 117–187.

Nibbering, N. M. M. ''Gas-phase reactions of organic anions.'' *Adv. Phys. Org. Chem.* **1988,** *24,* 1–55.

Freiser, B. S. ''Applications of FT/ICR spectrometry to the study of transition metal-containing ions in the gas phase.'' *Chemtracts—Analyt. & Phys. Chem.* **1989,** *1,* 65–109.

Ghaderi, S. ''Analysis of ceramics by laser ablation FTMS.'' *Ceram. Transactions* **1989,** *5,* 73–86.

Gord, J. R.; Freiser, B. S. ''Separation of experiments in time and space using dual-cell FT/ICR/MS.'' *Anal. Chim. Acta* **1989,** *225,* 11–24.

Marshall, A. G. ''Analytical capabilities and applications of FT/ICR mass spectrometry.'' *Adv. Mass Spectrom.* **1989,** *11A,* 651–668.

Nibbering, N. M. M. ''A view on some recent developments in mass spectrometry.'' *Adv. Mass Spectrom.* **1989,** *11A,* 101–125.

Sharpe, P.; Richardson, D. E. ''Applications of FT/ICR/MS in coordination chemistry.'' *Coord. Chem. Rev.* **1989,** *93,* 59–85.

Wilkins, C. L.; Chowdhury, A. K.; Nuwaysir, L. M.; Coates, M. L. ''FTMS: current status.'' *Mass Spectrom. Rev.* **1989,** *8,* 67–92.

Laude, D. A., Jr.; Hogan, J. D. ''High performance FTMS for chemical analysis.'' *Technisches Messen* **1990,** *57,* 155–159.

Lubman, D. M., Ed., *Lasers in Mass Spectrometry;* Oxford U. Press: New York, **1990,** 545 pp.

Marshall, A. G. ''Fourier transform ion cyclotron resonance mass spectrometry.'' *Spectroscopy* **1990,** *5,* 30.

Campana, J. E. ''Laser probe mass spectrometry.'' In *Proc. SPIE Applied Spectroscopy in Material Science;* International Society for Optical Engineering, Bellingham, WA, **1991,** 138–149.

Eller, K.; Schwarz, H. ''Organometallic chemistry in the gas phase.'' *Chem. Rev.* **1991,** *91,* 1121–1177.

Marshall, A. G.; Grosshans, P. B. ''Fourier transform ion cyclotron resonance mass spectrometry: The teenage years.'' *Anal. Chem.* **1991,** *63,* 215A–229A.

Nuwaysir, L. M.; Wilkins, C. L. ''Matrix-assisted laser desorption by FTMS.'' In *Proc. SPIE Applied Spectroscopy in Material Science;* International Society for Optical Engineering, Bellingham, WA, **1991,** 112–123.

Dunbar, R. C. ''Infrared radiative cooling of gas-phase ions.'' *Mass Spectrom. Rev.* **1992,** *11,* 309–339.

Jacoby, C. B.; Holliman, C. L.; Gross, M. L. ''FTMS: Features, principles, capabilities, and limitations.'' In *Mass Spectrometry in the Biological Sciences: A Tutorial;* Gross, M. L., Ed.; Kluwer Academic Publishers: Dordrecht, **1992,** 93–116.

Köster, C.; Kahr, M. S.; Castoro, J. A.; Wilkins, C. L. ''Fourier-transform mass spectrometry.'' *Mass Spectrom. Rev.* **1992,** *11,* 495–512.

Schweikhard, L.; Alber, G. M.; Marshall, A. G. ''FT/ICR of highly-charged atomic ions.'' *Physica Scripta* **1992,** *46,* 598–602.

Schweikhard, L.; Marshall, A. G. ''Excitation modes for Fourier transform ion cyclotron resonance mass spectrometry.'' *J. Am. Soc. Mass Spectrom.* **1993,** *4,* 433–452.

Holliman, C. L.; Rempel, D. L.; Gross, M. L. ''Detection of high mass-to-charge ions by FTMS.'' *Mass Spectrom. Rev.* **1994,** *13,* 105–132.

Vartanian, V. H.; Anderson, J. S.; Laude, D. A. ''Advances in trapped ion cells for FTICRMS.'' *Mass Spectrom. Rev.* **1995,** *14,* 1–19.

Freiser, B. S. ''Gas phase metal ion chemistry.'' *J. Mass Spectrom.* **1996,** *31,* 703–715.

APPENDIX B.

List of physical constants (Cohen and Taylor, 1996)

Elementary charge = $q = 1.60217733 \times 10^{-19}$ Coulombs $\pm$ 0.30 ppm = 4.80653×10^{-10} statcoulombs or esu so that 1 eV = $1.60217733 \times 10^{-19}$ J

Boltzmann constant = $k = 1.380658 \times 10^{-23}$ J K^{-1} $\pm$ 8.5 ppm

Molar gas constant = $R = 8.314510$ J mol^{-1} K^{-1} $\pm$ 8.4 ppm

Atomic mass unit = u = Da = $1.6605402 \times 10^{-27}$ kg $\pm$ 0.59 ppm

Avogadro constant = $N_A = 6.0221367 \times 10^{23}$ mol^{-1} $\pm$ 0.59 ppm

Electron mass = $9.1093897 \times 10^{-31}$ kg $\pm$ 0.59 ppm

Speed of light = $c = 2.99792458 \times 10^{8}$ m/s

Conversions: 1 eV/c^2 = $1.782662696 \times 10^{-36}$ kg = $1.073543836 \times 10^{-9}$ u $\pm$ 0.3 ppm

Precise masses of various common elements (Audi and Wapstra, 1995)

^{1}H = 1.00782503214 u $\pm$ 0.00035 μu (one standard deviation)

^{2}H = 2.01410177799 u $\pm$ 0.00036 μu

^{3}H = 3.0160492675 u $\pm$ 0.0011 μu

^{3}He = 3.01602930970 u $\pm$ 0.00086 μu

^{4}He = 4.0026032497 u $\pm$ 0.0010 μu

^{13}C = 13.0033548378 u $\pm$ 0.0010 μu

^{14}C = 14.0032419884 u $\pm$ 0.0040 μu

^{14}N = 14.00307400524 u $\pm$ 0.00086 μu

^{15}N = 15.00010889844 u $\pm$ 0.00092 μu

^{16}O = 15.9949146221 u $\pm$ 0.0015 μu

^{17}O = 16.999131501 u $\pm$ 0.22 μu

^{18}O = 17.999160419 u $\pm$ 0.9 μu

^{20}Ne = 19.9924401759 u $\pm$ 0.0020 μu

^{23}Na = 22.989769675 u $\pm$ 0.23 μu

^{28}Si = 27.9769265327 u $\pm$ 0.0020 μu

$^{31}P = 30.973761512$ u ± 0.20 μu
$^{32}S = 31.972070690$ u ± 0.12 μu
$^{34}S = 33.967866831$ u ± 0.11 μu
$^{39}K = 38.963706861$ u ± 0.3 μu
$^{40}Ar = 39.9623831232$ u ± 0.0030 μu

APPENDIX C. FURTHER READING

Books on FT-ICR

Asamoto, B. *Spectroscopy* **1988,** *3,* 38–46 (reviews industrial applications).

Buchanan, M. V., Ed. *Fourier Transform Mass Spectrometry: Evolution, Innovation, and Applications, ACS Symp. Series,* **1987,** *359,* 205 pp. (book with 11 contributed chapters on FT-ICR principles and applications).

FT-ICR special journal issues

Pardue, H. L. *Analyt. Chim. Acta 178; Special Issue: Fourier Transform Mass Spectrometry: Fundamental Aspects and Analytical Applications;* Pardue, H. L., Ed.; **1985,** 158 pp.

Comisarow, M. B.; Nibbering, N. M. M. *Int. J. Mass Spectrom. Ion Proc. 72, Special Issue: Fourier Transform Ion Cyclotron Resonance Mass Spectrometry;* Comisarow, M. B.; Nibbering, N. M. M., Ed.; **1986,** 222 pp.

Wilkins, C. L. *Trends in Analyt. Chem. 13, Special Issue: Fourier Transform Mass Spectrometry;* Wilkins, C. L., Ed.; **1994,** 223–251.

Marshall, A. G. *Int. J. Mass Spectrom. Ion Processes 137/138: Special Issue: Fourier Transform Ion Cyclotron Resonance Mass Spectrometry;* Marshall, A. G., Ed.; **1996,** 410 pp.

Complications of FT-ICR literature

Wanczek, K.-P. *Int. J. Mass Spectrom. Ion Proc.* **1984,** *60,* 11–60 (comprehensive ICR literature review to that date).

Wilkins, C. L.; Chowdhury, A. K.; Nuwaysir, L. M.; Coates, M. L. *Mass Spectrom. Rev.* **1989,** *8,* 67–92 (inclusive review of FT-ICR applications from 1986–88).

Dienes, T.; Pastor, S. J.; Schurch, S.; Scott, J. R.; Yao, J.; Cui, S.; Wilkins, C. L. *Mass Spectrom. Rev.* **1996,** *15,* 163–211 (comprehensive ICR literature review from 1992–mid-96).

Fourier transform techniques

Marshall, A. G.; Verdun, F. R. *Fourier Transforms in NMR, Optical, and Mass Spectrometry: A User's Handbook;* Elsevier: Amsterdam, **1990** (reasonably comprehensive description of analog and digital FT manipulations as applied to spectroscopy).

Early history of FT-ICR MS

Comisarow, M. B.; Marshall, A. G. *J. Mass Spectrom.* **1996,** *31,* 581–585 (review of the first FT-ICR MS experiments).

Marshall, A. G., *Acc. Chem. Res.* **1985,** *18,* 316–322 (historical review of the early development of FT-ICR mass spectrometry).

Gross, M. L.; Rempel, D. L. *Science* **1984,** *226,* 261–268 (review of early FT-ICR experiments).

ICR excitation

Schweikhard, L.; Marshall, A. G. *J. Am. Soc. Mass Spectrom.* **1993,** *4,* 433–452 (dipolar/quadrupolar, axial/cyclotron/magnetron excitation).

ICR signal generation and detection

Comisarow, M. B. *J. Chem. Phys.* **1978,** *69,* 4097–4104 (fundamental treatment of ICR signal generation in an infinitely extended ICR ion trap).

Limbach, P. A.; Grosshans, P. B.; Marshall, A. G. *Anal. Chem.* **1993,** *65,* 135–140 (determination of number of trapped ions in a cubic trap).

ICR line shape at low, intermediate, and high pressure

Marshall, A. G.; Comisarow, M. B.; Parisod, G. *J. Chem. Phys.* **1979,** *71,* 4434–4444 (fundamental relations between relaxation and FT-ICR spectral line shape).

SWIFT excitation

Guan, S.; Marshall, A. G. *Int. J. Mass Spectrom. Ion Processes* **1996,** *157/158,* 5–37 (comprehensive review).

Penning traps

Brown, L. S.; Gabrielse, G. ''Geonium theory. Physics of a single electron or ion in a penning trap.'' *Rev. Modern Phys.* **1986,** *58,* 233–311 (classic reference for the motions of an ion in an ideal Penning trap).

Guan, S.; Marshall, A. G. *Int. J. Mass Spectrom. Ion Processes* **1995,** *146/147,* 261–296 (comprehensive review).

Vartanian, V. H.; Anderson, J. S.; Laude, D. A. *Mass Spectrom. Rev.* **1995,** *14,* 1–19 (good discussion of open cylindrial traps).

External ion injection

Marshall, A. G.; Schweikhard, L. *Int. J. Mass Spectrom. Ion Processes* **1992,** *118/119,* 37–70 (reviews methods for guiding ions from an external ion source through the magnetic fringe field to the ICR Penning trap).

Ion-molecule chemistry from FT-ICR MS

Freiser, B. S. *Acc. Chem. Res.* **1994,** *27,* 353–360 (review of selected topics in organometallic ion chemistry studied by FT-ICR).

Green, M. K.; Lebrilla, C. B. *Mass Spectrom. Rev.* **1997,** *16,* 53–71 (review of ion-molecule reactions as probes of gas-phase structures of peptides and proteins).

Quadrupolar axialization

Guan, S.; Kim, H. S.; Marshall, A. G.; Wahl, M. C.; Wood, T. D.; Xiang, X. *Chem. Rev.* **1994,** *8,* 2161–2182 (comprehensive review of theory and applications).

Two-dimensional ICR

Haebel, S.; Gäumann, T. *Int. J. Mass Spectrom. Ion Proc.* **1995,** *144,* 139–166 (reviews Hadamard and Fourier transform methods for sorting out precursor/product ion connections for all precursor ions at once).

High Mass FT-ICR MS

Buchanan, M. V.; Hettich, R. L. *Anal. Chem.* **1993,** *65,* 245A–259A (review of FT-ICR mass spectrometry of high-mass biomolecules).

Holliman, C. L.; Rempel, D. L.; Gross, M. L. *Mass Spectrom. Rev.* **1994,** *13,* 105–132 (general discussion of problems associated with high *m*/*z* ions in FT-ICR).

Senko, M. W.; McLafferty, F. W. *Annu. Rev. Biophys. Biomol. Struct.* **1994,** *23,* 763–785 (review of mass spectrometry of large biomolecules).

CE FT-ICR MS

Hofstadler, S. A.; Severs, J. C.; Smith, R. D.; Swanek, F. D.; Ewing, A. G. *J. High Resol. Chromatogr.* **1996,** *19,* 617–621 (history and ''state-of-the-art'' for CE FT-ICR MS).

REFERENCES

1. Alber, G. M.; Marshall, A. G. ''Effect of sampling rate on Fourier transform spectra: oversampling is overrated.'' *Appl. Spectrosc.* **1990,** *44,* 1111–1116.
2. Alford, J. M.; Williams, P. E.; Trevor, D. J.; Smalley, R. E. ''Metal cluster ICR. Combining supersonic metal cluster beam technology with FT-ICR.'' *Int. J. Mass Spectrom. Ion Proc.* **1986,** *72,* 33–51.
3. Allemann, M.; Kellerhals, H.-P.; Wanczek, K.-P. ''Sidebands in the ICR spectrum and their application for exact mass determination.'' *Chem. Phys. Lett.* **1981,** *84,* 547–551.
4. Amster, I. J.; Loo, J. A.; Furlong, J. J. P.; McLafferty, F. W. ''Cesium ion desorption ionization with Fourier transform mass spectrometry.'' *Anal. Chem.* **1987,** *59,* 313–317.
5. Asamoto, B.; Dunbar, R. C. *Analytical Applications of Fourier Transform Ion Cyclotron Resonance Mass Spectrometry;* VCH: New York, **1991,** 306 pp.
6. Audi, G.; Wapstra, A. H. ''The 1995 update to the atomic mass evaluation.'' *Nuclear Physics A* **1995,** *595,* 409–425.
7. Beauchamp, J. L. ''Theory of collision-broadened ICR spectra.'' *J. Chem. Phys.* **1967,** *46,* 1231–1243.
8. Beu, S. C.; Laude, D. A., Jr. ''Elimination of axial ejection during excitation with a capacitively coupled open trapped-ion cell for FTICRMS.'' *Anal. Chem.* **1992a,** *64,* 177–180.
9. Beu, S. C.; Laude, D. A., Jr. ''Open trapped ion cell geometries for FT/ICR/MS.'' *Int. J. Mass Spectrom. Ion Proc.* **1992b,** *112,* 215–230.
10. Boering, K. A.; Rolfe, J.; Brauman, J. I. ''Control of ion kinetic energy in ion cyclotron resonance spectrometry: very-low-energy collision-induced dissociation.'' *Rapid Commun. Mass Spectrom.* **1992,** *6,* 303–305.
11. Bollen, G.; Moore, R. B.; Savard, G.; Stolzenberg, H. ''Quadrupole excitation for magnetron-to-cyclotron conversion.'' *Appl. Phys.* **1990,** *68,* 4355–4374.
12. Bowers, W. D.; Delbert, S.-S.; Hunter, R. L.; McIver, R. T., Jr. ''Fragmentation of oligopeptide ions using ultraviolet laser radiation and Fourier transform mass spectrometry.'' *J. Am. Chem. Soc.* **1984,** *106,* 7288–7289.
13. Caravatti, P.; Allemann, M. ''RF shim by trap segmentation.'' *Org. Mass Spectrom.* **1991,** *26,* 514–518.
14. Castoro, J. A.; Köster, C.; Wilkins, C. ''Matrix-assisted laser desorption/ionization of high-mass molecules by Fourier-transform mass spectrometry.'' *Rapid Commun. Mass Spectrom.* **1992a,** *6,* 239–241.
15. Castoro, J. A.; Nuwaysir, L. M.; Ijames, C. F.; Wilkins, C. L. ''Comparative study of photodissociation and surface-induced dissociation by laser desorption mass spectrometry.'' *Anal. Chem.* **1992b,** *64,* 2238–2243.
16. Castro, M. E.; Russell, D. H. ''Cesium ion desorption ionization with Fourier transform mass spectrometry.'' *Anal. Chem.* **1984,** *56,* 578–581.
17. Chen, R.; Cheng, X.; Mitchell, D. W.; Hofstadler, S. A.; Wu, Q.; Rockwood, A. L.; Sherman, M. G.; Smith, R. G. ''Trapping, detection, and mass determination of coliphage T4 DNA ions of 10^8 Da by electrospray ionization Fourier transform ion cyclotron resonance mass spectrometry.'' *Anal. Chem.* **1995,** *67,* 1159–1163.
18. Chiarelli, M. P.; Gross, M. L. ''FTMS for chemical analysis: A brief status report.'' In *Analytical Applications of Spectroscopy;* Creaser, C. S.; Davies, A. M. C., Ed.; Royal Society of Chemistry: London, **1988,** 262–273 pp.
19. Chorush, R. A.; Little, D. P.; Beu, S. C.; Wood, T. D.; McLafferty, F. W. ''Surface-induced dissociation of multiply-protonated proteins.'' *Anal. Chem.* **1995,** *67,* 1042–1046.
20. Cody, R. B.; Burnier, R. C.; Freiser, B. S. ''Collision-induced dissociation with Fourier transform mass spectrometry.'' *Anal. Chem.* **1982,** *54,* 96–101.
21. Cohen, E. R.; Taylor, B. N. ''The fundamental physical constants.'' *Physics Today* **1996,** *49,* BG9–BG13.
22. Comisarow, M. B. ''FT/ICR spectroscopy.'' *Adv. Mass Spectrom.* **1978a,** *7,* 1042–1046.
23. Comisarow, M. B. ''Signal modeling for ion cyclotron resonance.'' *J. Chem. Phys.* **1978b,** *69,* 4097–4104.
24. Comisarow, M. B. ''Fourier transform ion cyclotron resonance spectroscopy.'' *Adv. Mass Spectrom.* **1980,** *8,* 1698–1706.
25. Comisarow, M. B. ''Cubic trapped-ion cell for ion cyclotron resonance.'' *Int. J. Mass Spectrom. Ion Phys.* **1981,** *37,* 251–257.
26. Comisarow, M. B.; Marshall, A. G. ''Fourier transform ion cyclotron resonance spectroscopy.'' *Chem. Phys. Lett.* **1974a,** *25,* 282–283.
27. Comisarow, M. B.; Marshall, A. G. ''Frequency-sweep Fourier transform ion cyclotron resonance spectroscopy.'' *Chem. Phys. Lett.* **1974b,** *26,* 489–490.
28. Comisarow, M. B.; Marshall, A. G. ''Selective-phase ion cyclotron resonance spectroscopy.'' *Can. J. Chem.* **1974c,** *52,* 1997–1999.
29. Comisarow, M. B.; Marshall, A. G. ''Fourier transform ion cyclotron resonance spectroscopy method and apparatus.'' USA Patent No. 3,937,955, issued 14 February, 1976.
30. Comisarow, M. B.; Melka, J. ''Error estimates for finite zero-filling in Fourier transform spectroscopy.'' *Anal. Chem.* **1979,** *51,* 2198–2203.
31. Craig, E. C.; Santos, I.; Marshall, A. G. ''Dispersion vs. absorption (DISPA) method for automatic phase correction of Fourier transform ion cyclotron resonance mass spectra.'' *Rapid Commun. Mass Spectrom.* **1987,** *1,* 33–37.
32. Dehmelt, H. ''Ion traps.'' *Rev. Mod. Phys.* **1990,** *62,* 525–530.

33. Dunbar, R. C.; McMahon, T. B. ''Activation of unimolecular reactions by ambient blackbody radiation.'' *Science* **1998,** *279,* 194–197.
34. Elkind, J. L.; Weiss, F. D.; Alford, J. M.; Laaksonen, R. T.; Smalley, R. E. ''Fourier transform ion cyclotron resonance studies of H_2 chemisorption on niobium cluster cations.'' *J. Chem. Phys.* **1988,** *88,* 5215–5224.
35. Eller, K.; Schwarz, H. ''Organometallic chemistry in the gas phase.'' *Chem. Rev.* **1991,** *91,* 1121–1177.
36. Emmett, M. R.; Caprioli, R. M. ''Micro-electrospray mass spectrometry: ultra-high-sensitivity analysis of peptides and proteins.'' *J. Amer. Soc. Mass Spectrom.* **1994,** *5,* 605–613.
37. Emmett, M. R.; White, F. M.; Hendrickson, C. L.; Shi, S. D.-H.; Marshall, A. G. ''Application of micro-electrospray liquid chromatography techniques to FT-ICR MS to enable high sensitivity biological analysis.'' *J. Am. Soc. Mass Spectrom.* **1998,** *9,* 333–340.
38. Fenn, J. B.; Mann, M.; Meng, C. K.; Wong, S. F.; Whitehouse, C. M. ''Electrospray ionization for mass spectrometry of large biomolecules.'' *Science* **1989,** *246,* 64–71.
39. Freiser, B. S. ''Fourier transform mass spectrometry.'' In *Techniques for the Study of Ion Molecule Reactions;* Farrar, J. M.; Saunders, W. H., Jr., Ed.; Wiley: New York, **1988,** *20,* 61–118.
40. Freiser, B. S. ''Gas phase metal ion chemistry.'' *J. Mass Spectrom.* **1996,** *31,* 703–715.
41. Gabrielse, G.; Haarsma, L.; Rolston, S. L. ''Open-endcap Penning traps for high precision experiments.'' *Int. J. Mass Spectrom. Ion Processes* **1989,** *88,* 319–332.
42. Gauthier, J. W.; Trautman, T. R.; Jacobson, D. B. ''Sustained off-resonance irradiation for CAD involving FTMS. CAD technique that emulates infrared multiphoton dissociation.'' *Anal. Chim. Acta* **1991,** *246,* 211–225.
43. Goeringer, D. E.; Whitten, W. B.; Ramsey, J. M.; McLuckey, S. A.; Glish, G. L. ''Theory of high-resolution mass spectrometry achieved via resonance ejection in the quadrupole ion trap.'' *Anal. Chem.* **1992,** *64,* 1434–1439.
44. Grosshans, P. B.; Marshall, A. G. ''Theory of ion cyclotron resonance mass spectrometry: Resonant excitation and radial ejection in orthorhombic and cylindrical ion traps.'' *Int. J. Mass Spectrom. Ion Proc.* **1990,** *100,* 347–379.
45. Guan, S. ''Generation of optimal excitation pulses for two energy level systems using an inverse FT method.'' *J. Chem. Phys.* **1992,** *96,* 7959–7964.
46. Guan, S.; Marshall, A. G. ''Stored waveform inverse Fourier transform (SWIFT) axial excitation/ejection for quadrupole ion trap mass spectrometry.'' *Anal. Chem.* **1993,** *65,* 1288–1294.
47. Guan, S.; Kim, H. S.; Marshall, A. G.; Wahl, M. C.; Wood, T. D.; Xiang, X. ''Shrink-wrapping an ion cloud for higher-performance Fourier transform ion cyclotron resonance mass spectrometry.'' *Chem. Rev.* **1994,** *94,* 2161–2182.
48. Guan, S.; Marshall, A. G. ''Ion traps for FT-ICR/MS: Principles and design of geometric and electric configurations.'' *Int. J. Mass Spectrom. Ion Processes* **1995,** *146/147,* 261–296.
49. Guan, S.; Marshall, A. G.; Scheppele, S. E. ''Resolution and chemical formula identification of aromatic hydrocarbons containing sulfur, nitrogen, and/or oxygen in crude oil distillates.'' *Anal. Chem.* **1996,** *68,* 46–71.
50. Guan, S.; Marshall, A. G. ''Stored waveform inverse Fourier transform (SWIFT) ion excitation in trapped-ion mass spectrometry: Theory and applications.'' *Int. J. Mass Spectrom. Ion Processes* **1996,** *157/158,* 5–37.
51. Guan, S.; Marshall, A. G. ''Two-way conversation with a mass spectrometer: Non-destructive interactive mass spectrometry.'' *Anal. Chem.* **1997a,** *69,* 1–4.
52. Guan, S.; Marshall, A. G. ''Linear prediction Cholesky decomposition vs. Fourier transform spectral analysis for ion cyclotron resonance mass spectrometry.'' *Anal. Chem.* **1997b,** *69,* 1156–1162.
53. Guan, S.; Li, G.-Z.; Marshall, A. G. ''Effect of ion-neutral collision mechanism on trapped-ion equation of motion: A new mass spectral line shape for high-mass trapped ions.'' *Int. J. Mass Spectrom. Ion Processes* **1998,** *167/168,* 185–194.
54. Haebel, S.; Walser, M.-E.; Gäumann, T. ''High front-end resolution collision-induced dissociation in FT-ICR mass spectrometry.'' *Int. J. Mass Spectrom. Ion Proc.* **1995,** *151,* 97–115.
55. Hendrickson, C. L.; Drader, J. J.; Laude, D. A., Jr. ''Simplified application of quadrupolar excitation in Fourier transform ion cyclotron resonance mass spectrometry.'' *J. Am. Soc. Mass Spectrom.* **1995,** *6,* 448–452.
56. Henry, K. D.; Williams, E. R.; Wang, B.-H.; McLafferty, F. W.; Shabanowitz, J.; Hunt, D. F. ''Fourier-transform mass spectrometry of large molecules by electrospray ionization.'' *Proc. Natl. Acad. Sci. USA* **1989,** *86,* 9075–9078.
57. Henry, K. D.; McLafferty, F. W. ''Electrospray ionization with Fourier-transform mass spectrometry. Charge state assignment from resolved isotopic peaks.'' *Org. Mass Spectrom.* **1990,** *25,* 490–492.
58. Hettich, R. L.; Buchanan, M. V. ''Matrix-assisted laser desorption Fourier transform mass spectrometry for the structural examination of modified nucleic acid constituents.'' *Int. J. Mass Spectrom. Ion Proc.* **1991,** *111,* 365–380.
59. Hill, N. C.; Limbach, P. A.; Shomo, R. E., II; Marshall, A. G.; Appelhans, A. D.; Delmore, J. E. ''Fast neutral beam ion source coupled to a Fourier transform ion cyclotron resonance mass spectrometer.'' *Rev. Sci. Instrum.* **1991,** *62,* 2612–2617.
60. Hofstadler, S. A.; Laude, D. A., Jr. ''Trapping and detection of ions generated in a high magnetic field electrospray ionization Fourier transform ion cyclotron resonance mass spectrometer.'' *J. Amer. Soc. Mass Spectrom.* **1992,** *3,* 615–623.
61. Hofstadler, S. A.; Wahl, J. H.; Bruce, J. E.; Smith, R. D. ''On-line capillary electrophoresis with Fourier transform ion cyclotron resonance mass spectrometry.'' *J. Amer. Chem. Soc.* **1993,** *115,* 6983–6984.

62. Hofstadler, S. A.; Severs, J. C.; Smith, R. D.; Swanek, F. D.; Ewing, A. G. ''Analysis of single cells with capillary electrophoresis electrospray ionization Fourier transform ion cyclotron resonance mass spectrometry.'' *Rapid Comm. Mass Spectrom.* **1996,** *10,* 919–922.
63. Hop, C. E. C. A.; McMahon, T. B.; Willett, G. D. ''Determination of bond dissociation energies via energy-resolved CID in an FT/ICR spectrometer.'' *Int. J. Mass Spectrom. Ion Proc.* **1990,** *101,* 191–208.
64. Hsu, A. T.; Ricca, T. L.; Marshall, A. G. ''Clipped representations of Fourier transform ion cyclotron resonance mass spectra.'' *Anal. Chim. Acta* **1985,** *178,* 27–41.
65. Ijames, C. F.; Wilkins, C. L. ''Surface-induced dissociation by FT/ICR/MS.'' *Anal. Chem.* **1990,** *62,* 1295–1299.
66. Jackson, G.; Canterbury, J. D.; Guan, S.; Marshall, A. G. ''Linearity and quadrupolarity of tetragonal and cylindrical Penning traps of arbitary length-to-width ratio.'' *J. Amer. Soc. Mass Spectrom.* **1997a,** *8,* 283–293.
67. Jackson, G. S.; Hendrickson, C. L.; Reinhold, B. B.; Marshall, A. G. ''Two-plate vs. four-plate azimuthal quadrupolar excitation for FT-ICR mass spectrometry.'' *Int. J. Mass Spectrom. Ion Processes* **1997b,** *165/166,* 327–338.
68. Julian, R. K., Jr.; Cooks, R. G. ''Broad band excitation in the quadrupole ion trap mass spectrometer using shaped pulses with the inverse Fourier transform.'' *Anal. Chem.* **1993,** *65,* 1827–1833.
69. Kelleher, N. L.; Senko, M. W.; Siegel, M. M.; McLafferty, F. W. ''Unit resolution mass spectra of 112 kDa molecules with 3 Da accuracy.'' *J. Amer. Soc. Mass Spectrom.* **1997,** *8,* 380–383.
70. Kim, H. S.; Marshall, A. G. ''Magnitude-mode multiple-derivative spectra for resolution enhancement without loss in signal-to-noise ratio in Fourier transform mass spectrometry.'' *J. Mass Spectrom.* **1995,** *30,* 1237–1244.
71. Knight, R. D. ''The general form of the quadrupole ion trap potential.'' *Int. J. Mass Spectrom. Ion Proc.* **1983,** *51,* 127–131.
72. Kofel, P.; Allemann, M.; Kellerhals, H.; Wanczek, K.-P. ''Coupling of axial and radial motions in ICR cells during excitation.'' *Int. J. Mass Spectrom. Ion Proc.* **1986a,** *74,* 1–12.
73. Kofel, P.; Allemann, M.; Kellerhals, H.; Wanczek, K.-P. ''Time-of-flight ICR spectrometry.'' *Int. J. Mass Spectrom. Ion Processes* **1986b,** *72,* 53–61.
74. Kofel, P.; McMahon, T. B. ''A high pressure external ion source for FT/ICR spectrometry.'' *Int. J. Mass Spectrom. Ion Proc.* **1990,** *98,* 1–24.
75. Langevin, P. ''Une formule fondamentale de theorie cinetique.'' *Ann. Chim. Phys.* **1905,** *5,* 245.
76. Larsen, G. S.; Wronka, J.; Ridge, D. P. ''An ion cyclotron resonance spectrometer as a gas chromatographic detector. The effect of continuous trapping on performance.'' *Int. J. Mass Spectrom. Ion Processes* **1986,** *72,* 73–84.
77. Ledford, E. B., Jr.; Rempel, D. L.; Gross, M. L. ''Space charge effects in Fourier transform mass spectrometry. Mass calibration.'' *Anal. Chem.* **1984,** *56,* 2744–2748.
78. Lee, S. A.; Jiao, C. Q.; Huang, Y.; Freiser, B. S. ''Multiple excitation collisional activation in Fourier-transform mass spectrometry.'' *Rapid Commun. Mass Spectrom.* **1993,** *7,* 819–821.
79. Lee, S. H.; Wanczek, K.-P.; Hartmann, H. ''A new cylindrical trapped ion ICR cell.'' *Adv. Mass Spectrom.* **1980,** *8B,* 1645–1649.
80. Limbach, P. A.; Grosshans, P. B.; Marshall, A. G. ''Experimental determination of the number of trapped ions, detection limit, and dynamic range in FT/ICR/MS.'' *Anal. Chem.* **1993a,** *65,* 135–140.
81. Limbach, P. A.; Marshall, A. G.; Wang, M. ''An electrostatic ion guide for efficient transmission of low energy externally formed ions into a Fourier transform ion cyclotron resonance mass spectrometer.'' *Int. J. Mass Spectrom. Ion Proc.* **1993b,** *125,* 135–143.
82. Little, D. P.; Speir, J. P.; Senko, M. W.; O'Cornnor, P. B.; McLafferty, F. W. ''Infrared multiphoton dissociation of large multiply-charged ions for biomolecule sequencing.'' *Anal. Chem.* **1994,** *66,* 2809–2815.
83. Littlejohn, D. P.; Ghaderi, S. ''Mass spectrometer and method.'' USA Patent No. 4,581,533, issued 8 April, 1986.
84. Loo, J. F.; Krahling, M. D.; Farrar, T. C. ''Accurate ion abundance measurements in ICR/MS by linear prediction.'' *Rapid Commun. Mass Spectrom.* **1990,** *4,* 297–299.
85. Louris, J. N.; Brodbelt–Lustig, J. S.; Cooks, R. G.; Glish, G. L.; van Berkel, G. J.; McLuckey, S. A. ''Ion isolation and sequential stages of mass spectrometry in a quadrupole ion trap mass spectrometer.'' *Int. J. Mass Spectrom. Ion Proc.* **1990,** *96,* 117–137.
86. Lubman, D. M., Ed. *Lasers in Mass Spectrometry;* Oxford U. Press: New York, **1990,** 545 pp.
87. Marshall, A. G. ''Convolution Fourier transform ion cyclotron resonance spectroscopy.'' *Chem. Phys. Lett.* **1979,** *63,* 515–518.
88. Marshall, A. G. ''Ion cyclotron resonance and nuclear magnetic resonance spectroscopies: Magnetic partners for elucidation of molecular structure and reactivity.'' *Acc. Chem. Res.* **1996,** *9,* 307–316.
89. Marshall, A. G.; Comisarow, M. B.; Parisod, G. ''Relaxation and spectral line shape in Fourier transform ion cyclotron resonance spectroscopy.'' *J. Chem. Phys.* **1979,** *71,* 4434–4444.
90. Marshall, A. G.; Roe, D. C. ''Theory of Fourier transform ion cyclotron resonance mass spectroscopy: Response to frequency-sweep excitation.'' *J. Chem. Phys.* **1980,** *73,* 1581–1590.
91. Marshall, A. G.; Wang, T.-C. L.; Ricca, T. L. ''Tailored excitation for Fourier transform ion cyclotron resonance mass spectrometry.'' *J. Amer. Chem. Soc.* **1985,** *107,* 7893–7897.
92. Marshall, A. G.; Ricca, T. L.; Wang, T.-C. L. ''Tailored excitation for trapped ion mass spectrometry.'' USA Patent #4,761,545, issued 2 August 1988.
93. Marshall, A. G.; Verdun, F. R. *Fourier Transforms in*

NMR, Optical, and Mass Spectrometry: A User's Handbook; Elsevier: Amsterdam, **1990,** 460 pp.

94. Marshall, A. G.; Grosshans, P. B. ''Fourier transform ion cyclotron resonance mass spectrometry: The teenage years.'' *Anal. Chem.* **1991,** *63,* 215A–229A.
95. Marshall, A. G.; Guan, S. ''Advantages of high magnetic field for FT-ICR mass spectrometry.'' *Rapid Commun. Mass Spectrom.* **1996,** *10,* 1819–1823.
96. Marshall, A. G.; Senko, M. W.; Li, W.; Li, M.; Dillon, S.; Guan, S.; Logan, T. M. ''Protein molecular weight to 1 Da by ^{13}C, ^{15}N double-depletion and FT-ICR mass spectrometry.'' *J. Am. Chem. Soc.* **1997,** *119,* 433–434.
97. Marto, J. A.; Guan, S.; Marshall, A. G. ''Wide mass range axialization for high-resolution Fourier transform ion cyclotron resonance mass spectrometry of externally generated ions.'' *Rapid Commun. Mass Spectrom.* **1994,** *8,* 615–620.
98. McIver, R. T., Jr.; Hunter, R. L.; Bowers, W. D. ''Coupling a quadrupole mass spectrometer and a Fourier transform mass spectrometer.'' *Int. J. Mass Spectrom. Ion Processes* **1985,** *64,* 67–77.
99. McIver, R. T., Jr.; Li, Y.; Hunter, R. L. ''FTMS method for high resolution matrix-assisted laser desorption.'' *Int. J. Mass Spectrom. Ion Proc.* **1994,** *132,* L1–7.
100. McLafferty, F. W. ''High-resolution tandem FT mass spectrometry above 10 kDa.'' *Acc. Chem. Res.* **1994,** *27,* 379–386.
101. McLuckey, S. A.; Goeringer, D. E.; Glish, G. L. ''Selective ion isolation/ejection over a broad mass range in the quadrupole ion trap.'' *J. Am. Soc. Mass Spectrom.* **1991,** *2,* 11–21.
102. Meier, J. E.; Marshall, A. G. ''Bayesian versus Fourier spectral analysis of ion cyclotron resonance time-domain signals.'' *Anal. Chem.* **1990,** *62,* 201–208.
103. Meier, J. E.; Marshall, A. G. ''Pure absorption mode spectra from Bayesian maximum entropy analysis.'' *Anal. Chem.* **1991,** *63,* 551–560.
104. Mitchell, D.; Delong, S.; Cherniak, D.; Harrison, M. ''*z*-Axis oscillation sidebands in FT/ICR mass spectra.'' *Int. J. Mass Spectrom. Ion Proc.* **1989,** *91,* 273–282.
105. Mitchell, D. W.; Rockwood, A. L.; Chen, R.; Sherman, M. G.; Smith, R. D. ''Theoretical investigations of frequency shifts caused by electrostatic trapping field inhomogeneities in ion cyclotron resonance mass spectrometry.'' In *Proc. 42nd Amer. Soc. Mass Spectrom. Conf. on Mass Spectrom. & Allied Topics;* Amer. Soc. Mass Spectrom.: Chicago, IL, **1994,** 729.
106. Mitchell, D. W.; Smith, R. D. ''Cyclotron motion of two coulombically interacting ion clouds with implications to FT-ICR mass spectrometry.'' *Phys. Rev. E* **1995,** *52,* 4366–4386.
107. Mitchell, D. W.; Smith, R. D. ''Prediction of a space charge induced upper molecular mass limit towards achieving unit mass resolution in Fourier transform ion cyclotron resonance mass spectrometry.'' *J. Mass Spectrom.* **1996,** *31,* 771–790.
108. Nibbering, N. M. M. ''Gas-phase ion/molecule reactions as studied by FT/ICR.'' *Acc. Chem. Res.* **1990,** *23,* 279–285.
109. Pasa–Tolic, L.; Huang, Y.; Guan, S.; Kim, H. S.; Marshall, A. G. ''Ultrahigh-resolution matrix-assisted laser desorption/ionization Fourier transform ion cyclotron resonance mass spectrometry of peptides.'' *J. Mass Spectrom.* **1995,** *30,* 825–833.
110. Peiris, D. M.; Cheeseman, M. A.; Ramanathan, R.; Eyler, J. R. ''Infrared multiple photon dissociation spectra of gaseous ions.'' *J. Phys. Chem.* **1993,** *97,* 7839–7843.
111. Pfändler, P.; Bodenhausen, G.; Rapin, J.; Walser, M.-E.; Gäumann, T. ''2D FT/ICR/MS.'' *J. Amer. Chem. Soc.* **1988,** *110,* 5625–5628.
112. Price, W. D.; Schnier, P. D.; Jockusch, R. A.; Strittmatter, E. F.; Williams, E. R. ''Unimolecular reaction kinetics in the high-pressure limit without collisions.'' *J. Am. Chem. Soc.* **1996a,** *118,* 10640–10644.
113. Price, W. D.; Schnier, P. D.; Williams, E. R. ''Tandem mass spectrometry of large biomolecule ions by blackbody infrared radiative dissociation.'' *Anal. Chem.* **1996b,** *68,* 859–866.
114. Rempel, D. L.; Huang, S. K.; Gross, M. L. ''Relation of signal sensitivity and ion *z*-motion in cubic cells. Theory and implication for ion kinetic studies.'' *Int. J. Mass Spectrom. Ion Proc.* **1986,** *70,* 163–184.
115. Ross, C. W., III; Guan, S.; Grosshans, P. B.; Ricca, T. L.; Marshall, A. G. ''Two-dimensional Fourier transform ion cyclotron resonance mass spectrometry/mass spectrometry with stored-waveform ion radius modulation.'' *J. Amer. Chem. Soc.* **1993,** *115,* 7854–7861.
116. Schweikhard, L.; Marshall, A. G. ''Excitation modes for Fourier transform ion cyclotron resonance mass spectrometry.'' *J. Am. Soc. Mass Spectrom.* **1993,** *4,* 433–452.
117. Schweikhard, L.; Ziegler, J.; Bopp, H.; Lützenkirchen, K. ''The trapping condition and a new instability of the ion motion in the ion cyclotron resonance trap.'' *Int. J. Mass Spectrom. Ion Proc.* **1995,** *141,* 77–90.
118. Scott, W. T. ''Who was Earnshaw?'' *Am. J. Phys.* **1959,** *27,* 418–419.
119. Senko, M. W.; Beu, S. C.; McLafferty, F. W. ''Determination of monoisotopic masses and ion populations for large biomolecules from resolved isotopic distributions.'' *J. Amer. Soc. Mass Spectrom.* **1995,** *6,* 229–233.
120. Senko, M. W.; Hendrickson, C. L.; Pasa–Tolic, L.; Marto, J. A.; White, F. M.; Guan, S.; Marshall, A. G. ''Electrospray ionization FT-ICR mass spectrometry at 9.4 tesla.'' *Rapid Commun. Mass Spectrom.* **1996,** *10,* 1824–1828.
121. Senko, M. W.; Hendrickson, C. L.; Emmett, M. R.; Shi, S. D.-H.; Marshall, A. G. ''External accumulation of ions for enhanced electrospray ionization Fourier transform ion cyclotron resonance mass spectrometry.'' *J. Am. Soc. Mass Spectrom.* **1997,** *8,* 970–976.
122. Serreqi, A.; Comisarow, M. B. ''Frequency interpolation of discrete, apodized magnitude line shapes.'' *Appl. Spectrosc.* **1987,** *41,* 288–295.

123. Solouki, T.; Marto, J. A.; White, F. M.; Guan, S.; Marshall, A. G. ''Attomole biomolecule mass analysis by matrix-assisted laser desorption/ionization Fourier transform ion cyclotron resonance.'' *Anal. Chem.* **1995,** *67,* 4139–4144.

124. Solouki, T.; Pasa–Tolic, L.; Jackson, G. S.; Guan, S.; Marshall, A. G. ''High-resolution multistage MS, MS^2, MS^3 matrix-assisted laser desorption/ionization FT-ICR mass spectra of peptides from a single laser shot.'' *Anal. Chem.* **1996,** *68,* 3718–3725.

125. Soni, M. H.; Cooks, R. G. ''Selective injection and isolation of ions in quadrupole ion trap mass spectrometry using notched waveforms created using the inverse Fourier transform.'' *Anal. Chem.* **1994,** *66,* 2488–2496.

126. Soni, M.; Frankevich, V.; Nappi, M.; Santini, R. E.; Amy, J. W.; Cooks, R. G. ''Broad-band Fourier transform quadrupole ion trap mass spectrometry.'' *Anal. Chem.* **1996,** *68,* 3314–3320.

127. Speir, J. P.; Gorman, G. S.; Pitsenberger, C. C.; Turner, C. A.; Wang, P. P.; Amster, I. J. ''Remeasurement of ions using quadrupolar excitation Fourier transform ion cyclotron resonance spectrometry.'' *Anal. Chem.* **1993,** *65,* 1746–1752.

128. Speir, J. P.; Senko, M. W.; Little, D. P.; Loo, J. A.; McLafferty, F. W. ''High-resolution tandem mass spectra of 37-67 kDa proteins.'' *J. Mass Spectrom.* **1995,** *30,* 39–42.

129. Stacey, C. C.; Kruppa, G. H.; Watson, C. H.; Wronka, J.; Laukien, F. H.; Banks, J. F.; Whitehouse, C. M. ''Reverse-phase liquid chromatography/electrospray-ionization Fourier-transform mass spectrometry in the analysis of peptides.'' *Rapid Commun. Mass Spectrom.* **1994,** *8,* 513–516.

130. Steinfeld, J. I.; Francisco, J. S.; Hase, W. L. *Chemical Kinetics and Dynamics;* Prentice Hall: Englewood Cliffs, NJ, **1989.**

131. Stockton, G. W.; Meek, J. T.; Millen, W. G.; Wayne, R. S. ''An external ion source FT-ICR mass spectrometer for ultrahigh-mass accuracy measurements and high-performance liquid chromatographic sample introduction.'' In *FT-ICR/MS: Analytical Applications of Fourier Transform Ion Cyclotron Resonance Mass Spectrometry;* Asamoto, B., Ed.; VCH: New York, **1991,** 235–272.

132. Syka, J. E. P.; Fies, W. J., Jr. ''Fourier transform quadrupole mass spectrometer and method.'' USA Patent No. 4,755,670. **1988.**

133. Valaskovic, G. A.; Kelleher, N. K.; McLafferty, F. W. ''Attomole protein characterization by capillary electrophoresis-mass spectrometry.'' *Science* **1996,** *273,* 1199–1202.

134. Wang, B. H.; Amster, I. J.; McLafferty, F. W.; Brown, I. B. ''Metal-vapor vacuum arc as a primary ion source for secondary ion mass spectrometry.'' *Int. J. Mass Spectrom. Ion Proc.* **1990,** *100,* 51–61.

135. Wang, M.; Marshall, A. G. ''High-resolution multiple-ion simultaneous monitoring by means of multiple-foldover Fourier transform ion cyclotron resonance mass spectrometry.'' *Anal. Chem.* **1988,** *60,* 341–344.

136. Wang, T.-C. L.; Ricca, T. L.; Marshall, A. G. ''Extension of dynamic range in Fourier transform ion cyclotron resonance mass spectrometry via stored waveform inverse Fourier transform excitation.'' *Anal. Chem.* **1986,** *58,* 2935–2938.

137. Weast, R. C. *CRC Handbook of Chemistry and Physics;* CRC Press Inc.: Boca Raton, FL, **1989–1990.**

138. Williams, C. P.; Marshall, A. G. ''Hartley transform ion cyclotron resonance mass spectrometry.'' *Anal. Chem.* **1989,** *61,* 428–431.

139. Williams, C. P.; Marshall, A. G. ''Hartley/Hilbert transform spectroscopy: Absorption-mode resolution with magnitude-mode precision.'' *Anal. Chem.* **1992,** *64,* 916–923.

140. Williams, E. R.; McLafferty, F. W. ''Plasma desorption FT/ICR/MS.'' *J. Amer. Soc. Mass Spectrom.* **1990,** *1,* 427–430.

141. Williams, E. R.; Henry, K. D.; McLafferty, F. W. ''Remeasurement of heavy ions.'' *J. Amer. Chem. Soc.* **1990a,** *112,* 6157–6162.

142. Williams, E. R.; Henry, K. D.; McLafferty, F. W.; Shabanowitz, J.; Hunt, D. F. ''Surface-induced dissociation of peptide ions in FT/MS.'' *J. Am. Soc. Mass Spectrom.* **1990b,** *1,* 413–416.

143. Williams, E. R.; Loh, S. Y.; McLafferty, F. W.; Cody, R. B. ''Hadamard transform measurement of tandem FT mass spectra.'' *Anal. Chem.* **1990c,** *62,* 698–703.

144. Wobschall, D.; Graham, J. R., Jr.; Malone, D. P. ''ICR and the determination of collision cross sections.'' *Phys. Rev.* **1963,** *131,* 1565–1571.

145. Wood, T. D.; H., C. L.; Kelleher, N. L.; Little, D. P.; Kenyon, G. L.; McLafferty, F. W. ''Direct sequence data from heterogeneous creatine kinase (43 kDa) by high-resolution tandem mass spectrometry.'' *Biochemistry* **1995,** *34,* 16251–16254.

146. Woodlin, R. L.; Bomse, D. S.; Beauchamp, J. L. ''Multiphoton dissociation of molecules with low power continuous wave infrared laser radiation.'' *J. Am. Chem. Soc.* **1978,** *100,* 3248–3250.

147. Yin, W. W.; Wang, M.; Marshall, A. G.; Ledford, E. B., Jr. ''Experimental evaluation of a hyperbolic ion trap for FT/ICR/MS.'' *J. Amer. Soc. Mass Spectrom.* **1992,** *3,* 188–197.

148. Zhang, Z.; Guan, S.; Marshall, A. G. ''Enhancement of the effective resolution of mass spectra of high-mass biomolecules by maximum-entropy based deconvolution to eliminate the isotopic natural abundance distribution.'' *J. Am. Soc. Mass Spectrom.* **1997,** *8,* 659–670.

149. Zubarev, R. A.; Hakansson, P.; Sundqvist, B. ''Accuracy requirements for peptide characterization by monoisotopic molecular mass measurements.'' *Anal. Chem.* **1996,** *68,* 4060–4063.